SPACE-BORNE OBSERVATIONS OF THE LIFECYCLE OF INTERSTELLAR GAS AND DUST

EWINE F. VAN DISHOECK
Leiden Observatory, P.O. Box 9513
2300 RA Leiden, The Netherlands

AND

ALEXANDER G.G.M. TIELENS
SRON/Kapteyn Astronomical Institute, P.O. Box 800
9700 AV Groningen, The Netherlands

1. Introduction

The gas and dust in the interstellar medium (ISM) form an essential part of the evolution of galaxies, the formation of stars and planetary systems and the synthesis of organic molecules which may lead to the emergence of life elsewhere in the universe. Over their lifetime, stars return much of their mass to the ISM through winds and supernova explosions, leading to a slow enrichment in heavy elements and dust which form the building blocks from which future generations of stars and planets are made. Stars also inject energy into the ISM by ultraviolet photons, shocks and wind–blown stellar bubbles. Cosmic rays, X-rays and ionizing photons influence the ionization state of the gas, whereas shielding by gas and dust leads to the cold neutral phases of the ISM where molecules can flourish. As a result, the composition and structure of the ISM is a complex interplay of microscopic and macroscopic processes. Understanding this lifecycle of gas and dust in the ISM is a key problem in astrophysics, not only within our own galaxy but also for understanding the much more rapid cycling between the ISM and stars in the earliest star-forming galaxies in the universe (Figure 1).

Research on the ISM started early in the $20^{\rm th}$ century, with the ground-based detection of interstellar Na and Ca^+ optical absorption lines (Hartmann 1904, Heger 1919) and the appearance of many dark regions on photographic surveys of the Milky Way (e.g., Barnard 1919). Definite evidence for the presence of interstellar dust came from observations by Trumpler

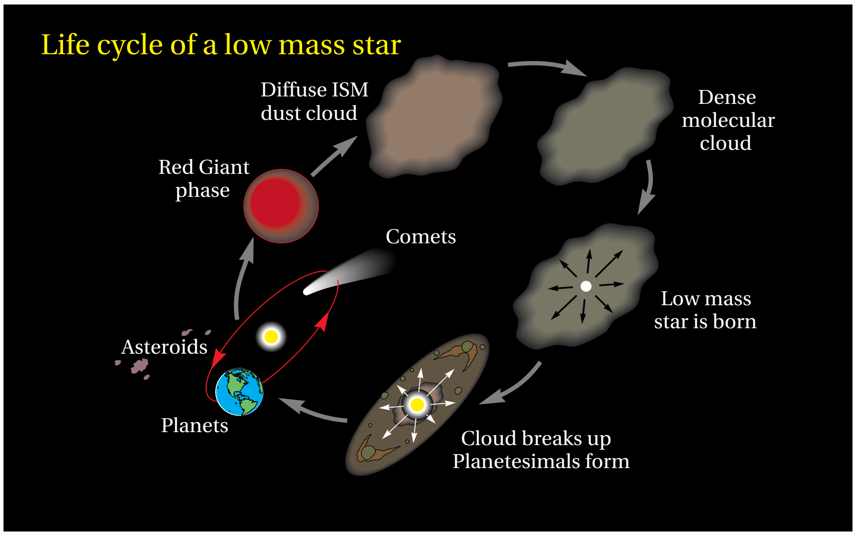

Figure 1. *Schematic diagram showing the lifecycle of dust and gas from the diffuse medium through star-formation and the late stages of stellar evolution (Pendleton & Cruikshank 1994).*

(1930), whereas the first interstellar molecules CH, CH^+ and CN were identified between 1937 and 1941 (Swings & Rosenfeld 1937, McKellar 1940, Douglas & Herzberg 1941). Around the same time, the Diffuse Interstellar Bands (DIBs) were detected (Heger 1922, Merrill 1934), whose identification is still a riddle after more than 75 years. Initially, inspired by the identification of simple diatomics in the ISM, these bands were attributed to molecular absorbers. However, once interstellar dust was established as an important interstellar component, an origin for the DIBs in absorption by dust grains was taken for granted. Nowadays, the pendulum has swung back – and for good reasons – to molecules as the prime candidates for the carriers of these absorption features (Snow 1995). The foundation of the theoretical study of the ISM and the physical conditions that may prevail was put forward by Eddington (1926) in his famous Bakerian lecture. Of course, Eddington was also the one to exclaim that "atoms are physics but molecules are chemistry" with the scarcely hidden message that astronomers should keep far from molecules. Nowadays, despite Eddington's dire warnings, molecular astrophysics is a thriving field driven to a large extent by the wealth of molecular data which has become available over the last three decades, much of it space–based.

With the detection of the H I 21 cm line by Ewen & Purcell (1951), the study of the ISM turned to ground-based radio observations and such data still provide a wealth of information on the distribution and kinematics of the neutral atomic ISM in our Galaxy and other galaxies (e.g., Hartmann & Burton 1997). The detection of the first molecules at radio wavelengths (Weinreb et al. 1963, Cheung et al. 1968) paved the way for the development of millimeter and submillimeter wave astronomy. The ubiquitous CO molecule was detected by Wilson et al. (1970) and a surprisingly large suite of other molecules has since been found in dense molecular clouds (see van Dishoeck & Hogerheijde 1999 for a recent overview).

Space-based ultraviolet observations of the neutral ISM started with small spectrometers flown on rockets, which led to the important detection of H_2 by Carruthers (1970). The subsequent Copernicus satellite (Spitzer & Jenkins 1975) provided extensive new information on H_2 and other interstellar lines, mostly of atoms in various ionization stages. Together with the ground-based H I data, they stimulated the development of the two- and three-phase model of the ISM, in which the gas is heated by the photoelectric effect on grains and large-scale supernova explosions, and is cooled by line radiation from atoms (Field, Goldsmith & Habing 1969, McKee & Ostriker 1977).

Because the typical temperatures of the cold, neutral ISM range from $\sim$10 K to a few hundred K, most of the thermal emission occurs at mid- and far-infrared wavelengths, a part of the spectrum which is largely obscured from the ground. It is therefore not surprising that much of our progress over the last 30 years or so resulted from space-based observations in the infrared. To our knowledge, the oldest discussion on the importance of the infrared for the study of the ISM goes back to an exchange by Spitzer, Kahn and Drake at the 3rd Symposium on Cosmical Gas Dynamics (Burges & Thomas 1958). Of course, the first detection of infrared radiation (from the Sun) was by William Herschel in 1800, while his son John Herschel was the first to measure the total power emitted by the Sun in 1838 and E. Stone that of stars in 1869–1870 (see Harwit 1999). Around the same time, Edison observed Arcturus and the solar corona in the infrared in a chicken coop in order to win a bet in the late 1870's (Eddy 1972). However, despite this impressive early success, the field of infrared astronomy was dormant until the late 1960's–early 1970's when progress in infrared instrumentation truly opened the infrared window of the spectrum.

The 1958 discussion quoted above went on to consider the observational difficulties of detecting a low intensity astronomical signal against a 300 K telluric background and emphasized the advantage of balloon or satellite observations. This was elaborated upon in an early discussion on infrared radiation from interstellar grains by Stein (1967) who concluded that it

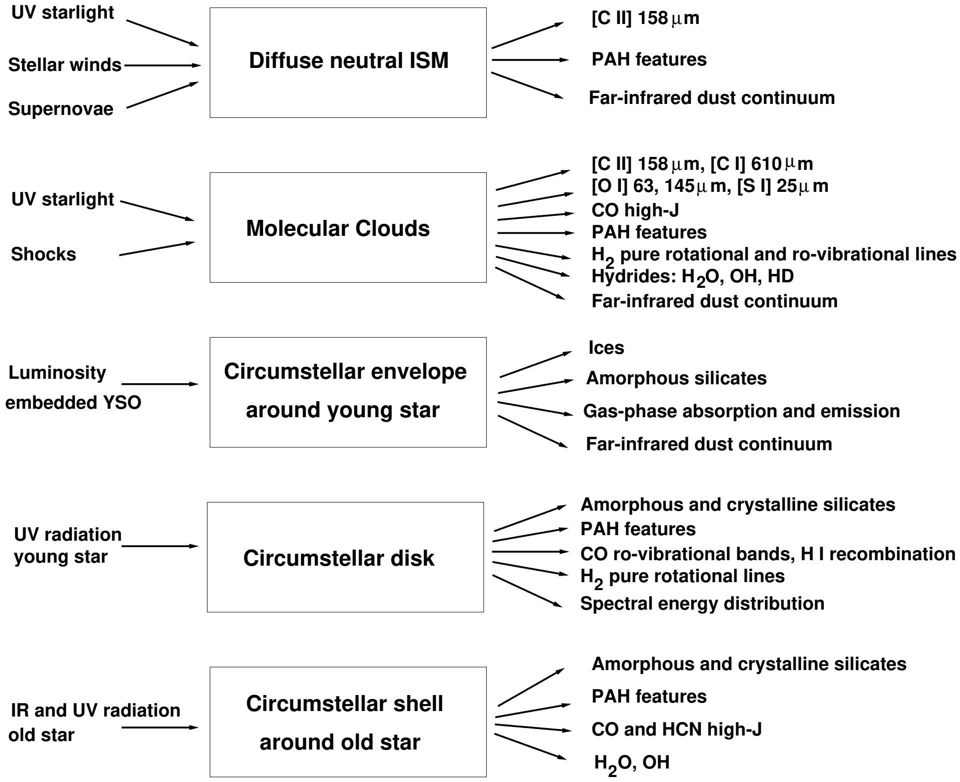

Figure 2. *Schematic diagram showing the energy input to the various phases of the interstellar medium discussed here and the resulting diagnostic lines at mid- and far-infrared wavelengths. Most of these features can only be observed from air- and space-borne platforms. PAH stands for Polycyclic Aromatic Hydrocarbons or large carbonaceous molecules in general.*

was hopeless to even consider observing it through the mid–infrared telluric windows. Fortunately, he was not much impressed with his own dire predictions and together with (among others) Fred Gillett he actually pioneered the field of mid-infrared spectroscopy of interstellar dust using a circular variable filterwheel. By the early 1970's, it was well realized that the best way to determine the composition of interstellar dust was through infrared spectroscopy (Gaustad 1971). That was an impressive foresight and insight as well as a change of directions in a short time. Remember that by the late 1960's and early 1970's, rocket–borne ultraviolet studies had revealed the ubiquitous presence of H_2 (Carruthers 1970) and of the 2200 Å bump in the interstellar extinction curve (Stecher 1965, Bless & Savage 1972) which had been successfully modeled by small graphite grains (Gilra

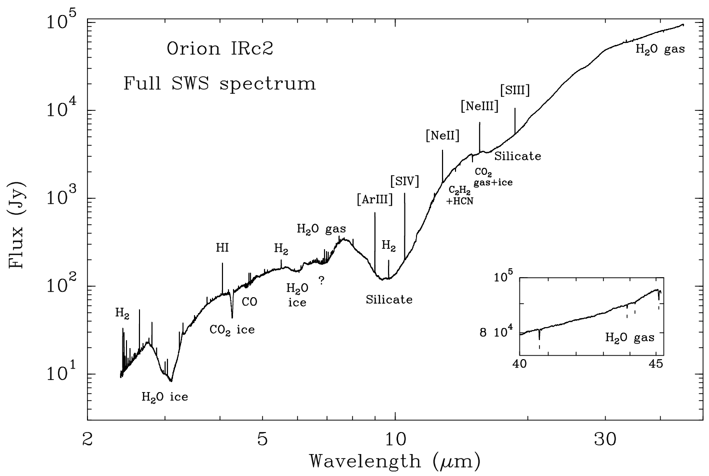

Figure 3. *Complete ISO–SWS grating spectrum centered on Orion IRc2 at a resolving power R=1300–2500. The SWS aperture ranges from* $14'' \times 20''$ *at 2 μm to* $20'' \times 27''$ *at 45 μm. The principal absorption and emission features are indicated. The inset shows a blow-up of the 40–45 μm region, in which several gas-phase* H_2O *absorption lines can be seen (van Dishoeck et al. 1998).*

1972).

Yet, as has become abundantly clear over the years since then, our knowledge on the physics and composition of the dust and gas has truly been driven by the advances in infrared detector and heterodyne submillimeter receiver technology, and by the development of airborne and space-based platforms through pioneers such as Martin Harwit, Gerard Kuiper, Frank J. Low, Charles H. Townes and many others (e.g., Harwit et al. 1966, Kleinmann & Low 1967). The Lear Jet and the Kuiper Airborne Observatory (KAO) in the US, and the US-NL-UK Infrared Astronomical Satellite (IRAS) have been pivotal in developing the field, which has culminated with ESA's recent Infrared Space Observatory (ISO) (see Table 1). Other important mission include the NASA Cosmic Background Explorer (COBE), balloons, rockets, the Japanese Infrared Telescope in Space (IRTS), the US Air-Force project MSX and the NASA Submillimeter Wave Astronomical Satellite (SWAS). In that respect, the future looks very promising with the Space InfraRed Telescope Facility (SIRTF), the ASTRO-F mission, the Far InfraRed and Submillimeter Telescope (FIRST), and the Next Generation Space Telescope (NGST) on the horizon.

In this chapter, an overview is given of the air- and space-borne observations over the last 30 years which have played a crucial role in our understanding of the cold and dense neutral interstellar medium and the

TABLE 1. Selected infrared space missions and instruments relevant for ISM research

Mission	Instrument	Acronym	Wavelength range (μm)	Resolving power	Operational period
IRAS	Photometers		12, 25, 60, 100	3–5	1983
	Low Resolution Spectrometer	LRS	7.7–22.6	20–60	
COBE	Far-InfraRed Absolute Spectrophotometer	FIRAS	100–10000	100–500	1989–1993
IRTS	Far Infrared Line Mapper	FILM	63, 158	400	1995
ISO	Short Wavelength Spectrometer	SWS	2.5–45	2000, 20000	1995-1998
	Long Wavelength Spectrometer	LWS	43–197	200, 10000	
	Camera	CAM	2.5–17	3–20	
	Camera+Circular Variable Filter	CAM-CVF	2.3–16.5	35–50	
	Photometer	PHT	3.3–200	3	
	Photometer-Spectrometer	PHT-S	2.5–5, 6–12	90	
SWAS	Heterodyne Instrument		545, 610	5×10^5	1999–

formation of stars. The various phases of the ISM discussed here are summarized in Figure 2, and are discussed in order from the diffuse medium to old stars. The richness of the infrared wavelength region is illustrated in Figure 3, which contains the complete ISO Short Wavelength Spectrometer (SWS) spectrum of Orion centered at the IRc2 source (van Dishoeck et al. 1998). Due to its proximity and extraordinary brightness, it has been the prime target for most of the pioneering observations at infrared wavelengths (e.g., Genzel & Stutzki 1989). Much of the complexity is the result of the disruption of the star-forming environment by powerful outflows from the massive young star and its intense ultraviolet radiation dissociating and ionizing the gas on the cloud surfaces. Orion is the nearest, best studied region of massive star formation in the Galaxy, and therefore also serves as an important template for more distant star-forming regions in external galaxies. The strong continuum is due to thermal emission from warm dust (50–300 K) and peaks around 70 μm. Superposed a wealth of lines of atoms, ions and molecules is seen, which can be used to constrain the physical parameters (see Figure 8 of Genzel 1992) and assess the importance of different processes, in particular shocks versus ultraviolet radiation.

Due to page limits, a comprehensive review of the field is not possible, and only topics in which space-based observations have played a crucial role are included. For example, ground-based submillimeter observations of molecular clouds are not covered, but the composition of ices in such clouds deduced from mid-infrared spectroscopy is. Ultraviolet observations of the atomic component of the ISM and space-based data on ionized H II regions and continuum observations of young stars are discussed elsewhere in this volume. Each section starts with a brief historical review and introduction of the basic physics, but then focuses on recent ISO results to illustrate the current state of knowledge, in particular the spectroscopic data obtained with the Short Wavelength Spectrometer (SWS, 2.4–45 μm) and Long Wavelength Spectrometer (LWS, 43–197 μm) (see Table 1 for overview). Excellent previous summaries include the proceedings of the *Airborne Astronomy Symposium* (Haas et al. 1995), which also contains many photographs of key people in the field, and the proceedings of the *The Diffuse Infrared Radiation and the IRTS* (Okuda et al. 1997). Further details of ISO results are contained in *Star Formation with the ISO Satellite* (Yun & Liseau 1998), *ISO's View on Stellar Evolution* (Waters et al. 1998), *Analytical Spectroscopy with ISO* (Heras et al. 1997, 2000), *Solid Interstellar Matter: The ISO Revolution* (d'Hendecourt et al. 1999a) and *The Universe as seen by ISO* (Cox & Kessler 1999). Reviews on various aspects of the neutral ISM include Spitzer (1978), Habing (1988), Genzel (1992), and Hollenbach & Tielens (1999), whereas recent reviews of astrochemistry can be found in *The Molecular Astrophysics of Stars and Galaxies* (Hartquist & Williams 1998), van Dishoeck & Blake (1998), van Dishoeck & Hogerheijde (1999), Langer et al. (2000), Ehrenfreund & Charnley (2000) and the proceedings of IAU Symposium 197 on *Astrochemistry: From Molecular Clouds to Planetary Systems* (Minh & van Dishoeck 2000). Interstellar dust has been reviewed by, e.g., Tielens & Allamandola (1987a,b), Whittet (1992) and Cox et al. (2000).

2. Diffuse Interstellar Medium

2.1. PRESENCE OF VERY SMALL GRAINS

The infrared emission from dust in the diffuse neutral ISM is faint and extended, and observations have been mostly limited to cooled telescopes from space. The all-sky maps by IRAS at 12, 25, 60 and 100 μm and COBE have been particularly important in revealing the spatial distribution of the dust in the Galaxy as well as the spectral energy distribution from near-infrared to millimeter wavelengths (Sodroski et al. 1994, Reach et al. 1995, see Figure 4). The IRAS 100 μm emission is due to thermal emission at $T \approx$18 K from big $\sim$0.1 μm-sized grains, and correlates well with the ground-based H I 21 cm emission in regions far removed from molecular clouds. This confirms that the dust and gas in these 'infrared cirrus' clouds are well mixed and that the heating of dust is quite homogeneous away from the galactic plane (e.g., Boulanger & Pérault 1988). Polarization observations of dust

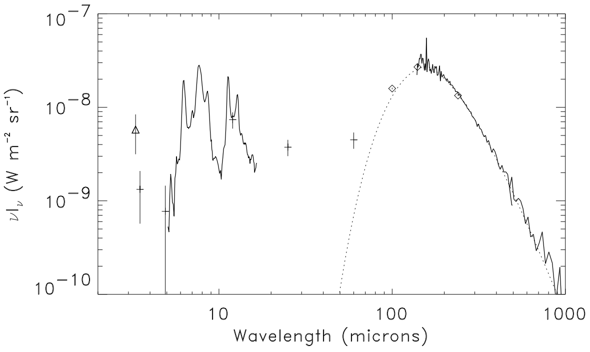

Figure 4. The dust emission spectrum from the near-infrared to millimeter wavelengths normalized for a column density of $10^{20}\,\mathrm{H\,cm^{-2}}$. *This figure combines (1) the* $3.3\mu\mathrm{m}$ *emission of cirrus associated with the molecular ring (Giard et al. 1994), (2) an ISO-CAM spectrum between 5 and 16* μm *of the diffuse Galactic emission at* $l{=}28^\circ$ *and* $b = 0.8^\circ$, *(3) measurements of the high latitude cirrus emission from the COBE satellite with the Diffuse Infrared Background Experiment (DIRBE) (Bernard et al. 1994) and the Far Infrared Absolute Spectrometer (FIRAS) (Boulanger et al. 1996). The dotted line represents the radiation from a modified black-body at a temperature* $T_{\rm dust} = 17.5\,K$ *with an emissivity law proportional to* ν^2. *The peak at* $158\,\mu\mathrm{m}$ *is a detection of the [C* II*] line from high latitude gas (Boulanger 1999).*

at optical (Hall 1949, Hiltner 1949) and far-infrared (e.g., Hildebrand et al. 1984, 1995) wavelengths show that the grains are non-spherical and aligned by the magnetic field.

In contrast, the strong and wide-spread 12 and 25 μm IRAS emission in cirrus clouds provided a puzzle initially. Sellgren (1984) proposed that such strong mid-infrared emission is due to very small dust grains, where absorptions of individual photons lead temporarily to much higher grain temperatures because of the limited heat capacity of small grains. The presence of small ($<$ 10 Å) grains in the ISM had been first proposed in 1956 by Platt to explain optical extinction and polarization, which was extended by Donn (1968) to ultraviolet extinction. This proposal was revived by Andriesse (1978) in a study of the infrared emission from H II regions. However, none of these insightful suggestions gained wide acceptance because other explanations were favored by Occam's razor: $\sim$ 1000 Å dielectric dust grains for the optical extinction and polarization, $\sim$ 200 Å graphite grains for the ultraviolet extinction, and heating of $\sim$ 100 Å grains by Ly α radiation for the mid–infrared emission from H II regions.

Temperature fluctuations of small grains had been considered by Greenberg & Hong (1974) and Purcell (1976) in connection with the formation (or prevention) of ice mantles, but the possible general importance for the

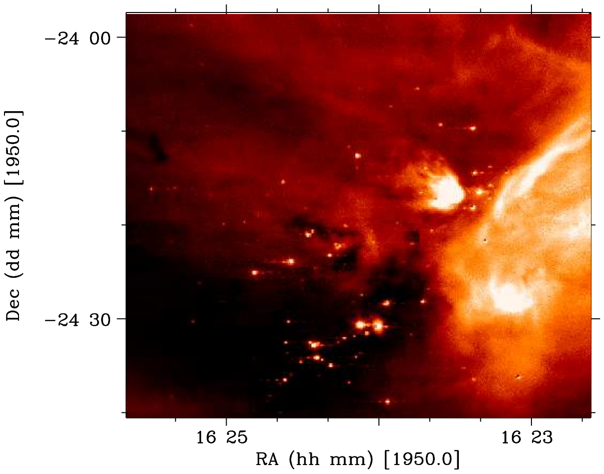

Figure 5. *ISO-CAM composite 6 and 15 μm image of the ρ Ophiuchi molecular cloud. The bright filaments in the West trace hot dust illuminated by the B2V star HD 147889, located just outside the map. The actual dense cloud is to the East. The dark patches are very dense clumps which are optically thick even at 15 μm, whereas the bright spots throughout the image are low and intermediate mass protostars. Most of the extended 6 μm emission is due to PAHs (Abergel et al. 1996).*

mid-infrared emission from the ISM had not been noticed. After the IRAS discovery of widespread galactic cirrus, this process has been studied in more detail by Draine & Anderson (1985), who showed that these temperature fluctuations contribute to the IRAS 60 μm emission as well. The IRAS 12–100 μm data have led to the development of new grain models, such as those by Désert et al. (1990) and Rowan-Robinson (1992). As will be discussed in §3.2, the very small grains seen by IRAS at 12 and 25 μm form part of a distribution of grain sizes ranging from large molecules such as Polycyclic Aromatic Hydrocarbons (PAHs) to big grains. ISO-PHOT and ISO-CAM (see Table 1) have demonstrated that the spectrum of the mid–infrared cirrus is dominated by the PAH bands (cf., §3.2, Mattila et al. 1996, see Figure 4). Likewise, spectral–imaging studies done with ISO-CAM on board of ISO have revealed that the surfaces of dark clouds are set aglow in these PAH bands by the impinging FUV photons (see Figure 5).

2.2. AMORPHOUS SILICATES AND HYDROCARBON DUST

Mid-infrared spectroscopy of the cold dust along the line of sight toward bright background sources can provide direct information on the composi-

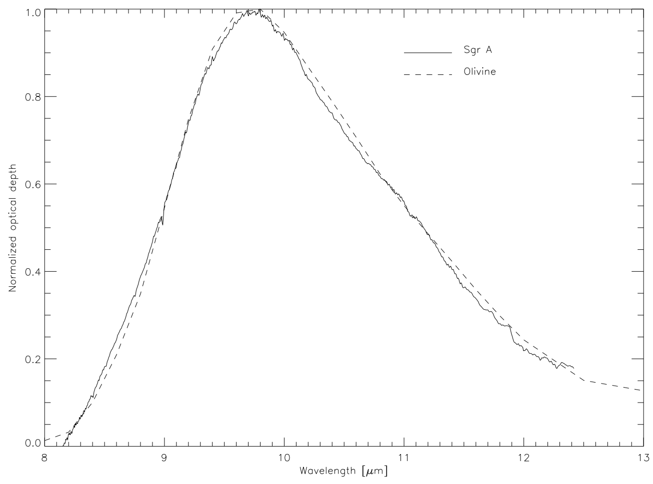

Figure 6. *The 10μm silicate optical depth observed toward the galactic center with the ISO-SWS. The dashed line is the laboratory spectrum of the amorphous olivine* $FeMgSiO_4$*. The broad feature around 10.5 μm may be due to residual detector memory effects (Vriend 2000).*

tion of the interstellar grains. The absorption spectra are dominated by the broad and strong 10 and 18 μm Si-O stretching and O-Si-O bending features of silicate dust, first detected by Gillett and coworkers (Gillett & Forrest 1973, Gillett et al. 1975). As an example, Figure 6 shows the 10 μm profile observed toward the galactic center Sgr A* with the ISO-SWS (Vriend 2000). This bright background source suffers some 30 magnitudes of visual extinction and is a prime target for the study of interstellar dust in the diffuse and translucent medium. The observed profile is remarkably smooth and shows no evidence for spectral substructure due to crystalline silicate components, expected for example at 11.3 μm. The crystalline/amorphous silicate ratio in the ISM must be less than a few percent (see also Demyk et al. 1999). This is in stark contrast with dust around young stellar objects (YSOs), solar system comets, massive supergiants, or some asymptotic giant branch (AGB) and post–AGB objects, which show up to 75 % crystalline silicate material (cf., §8.1). The observed 10 μm band is remarkably well fit by the laboratory spectrum of amorphous olivine with Fe/Mg $\simeq$1 (ie., $FeMgSiO_4$). However, the profile of the 18 μm band implicates also pyroxenes (i.e., $Fe_xMg_{(1-x)}SiO_3$) and this issue has not yet been settled completely. The lack of crystalline material suggests rapid processing of the grains in the ISM, perhaps through the bombardment with cosmic rays.

Hydrocarbon grains have been detected in the ISM through absorption in the C-H stretching mode at 3.4 μm from the ground (e.g., Wickramasinghe & Allen 1980, Pendleton et al. 1994). While the origin of this band in the CH stretching mode of aliphatic hydrocarbon (e.g., -CH_3 and -CH_2 groups) materials is well established, the precise nature of this carbonaceous material is still uncertain and many candidates have been proposed, including Hydrogenated Amorphous Carbon (HAC), Quenched Carbonaceous Carbon (QCC) and ultraviolet processed organic refractory grain mantles, leading to a lively debate in the community (cf., Martin 1989).

This discussion centers largely on the origin and evolution of interstellar dust and as such is really a continuation of a historical controversy which started in the early 1960's. One camp holds that interstellar dust is formed in stellar ejecta and consists therefore mainly of very refractory materials such as silicates and graphite (cf., Mathis et al. 1977). The other side maintains that interstellar dust is also formed through accretion and processing of icy grain mantles in the ISM itself (Greenberg 1982, Li & Greenberg 1997). Interstellar ice formed through accretion and reaction in the ISM was among the first dust models, originally proposed by van de Hulst (1949) in response to a prize essay contest on the origin and growth of solid particles in the ISM organized by Kramers and Oort at Leiden University during the war years (van de Hulst 1997). While this model had attractive features and was overall well received, the problem of nucleation at the low densities of the ISM was recognized. Moreover, by the early 1970's, the expected 3 μm ice band had not been observed in the diffuse ISM (cf., §5). The stardust model first saw light when Hoyle & Wickramasinghe (1962) surmounted the nucleation problem by proposing that dust forms at the high densities associated with stellar photospheres and is subsequently expulsed into space by radiation pressure. They focussed on graphite as a likely dust candidate, produced in C-rich giants, but later on it was concluded that oxides and silicates could form around O–rich giants (Kamijo 1963). By the late 1960's, this model was well supported by the discovery of infrared emission from warm, circumstellar dust grains around red giants and by the observed ubiquity of the 2200 Å feature in the interstellar extinction curve which is well fitted by graphitic-like grains. At present, there is no doubt that stardust formed in stellar ejecta is an important component of interstellar dust: genuine stardust grains which can be traced back to AGB stars have been found in meteorites in our laboratories (Anders & Zinner 1993)!

The KAO and ISO have provided further constraints on the composition of interstellar hydrocarbon grains through their study of the 5–8 μm region. This spectral region, which is obscured by telluric absorption, is very characteristic for C=C, C-C, C=O stretching modes and CH deformation

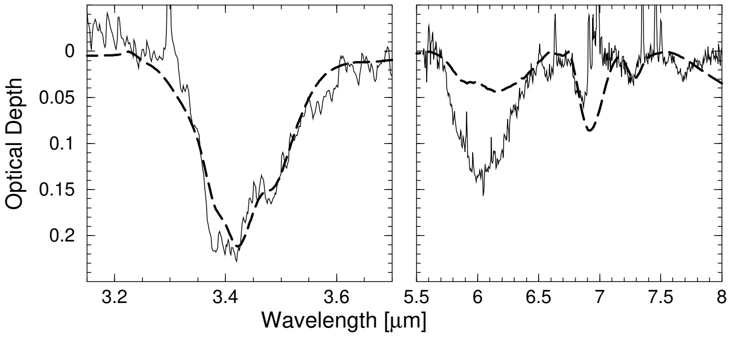

Figure 7. *The ISO-SWS 3.2–3.7 (left) and 5.5–8.0 μm (right) spectra of SgrA* on an optical depth scale, revealing weak absorption features which are well fitted in peak position and relative strength by the C-H stretching and deformation modes in Hydrogenated Amorphous Carbon. Most of the feature at 6.0 is due to H_2O ice while the 7.7 μm feature is due to CH_4 ice, discussed in §5 (Chiar et al. 2000).*

modes. The spectra show that the hydrocarbon dust component is largely carbon–based and contains very little oxygen (Tielens et al. 1996, Schutte et al. 1999, Chiar et al. 2000). The observed weak CH deformation modes at 6.85 and 7.3 μm compare well in relative strength and peak position with laboratory spectra of HAC – a refractory carbonaceous material analogous to high temperature soot – originally proposed by Duley & Williams (1983) (Figure 7; Chiar et al. 2000). Moreover, there is little evidence for the strong C=O modes which dominate the spectra of first-generation processed ice mantles (Greenberg & Muñoz-Caro 2000). Thus, if interstellar mantles play an important role in the ISM, the processing has to convert them almost completely from oxygen–dominated volatile ice mantles (cf., §5) to carbon–based refractory mantles and experimental studies have so far been unable to achieve this in the laboratory. The stardust model is not without problems either, however. In particular, stardust proponents still have to come to grips with the short dust lifetimes implied both by observations of interstellar depletion variations and by theoretical calculations which imply an active gas–grain interaction in the ISM (see review by Tielens 1999).

2.3. THE [C II] EMISSION FROM THE MILKY WAY

In addition to studies of dust, the space-based data provide information on the gas in the diffuse medium. The [C II] emission from the Galaxy has been studied using the FIRAS instrument on COBE and the Japanese balloon-borne BICE instrument (Figure 8; Wright et al. 1991, Bennett et al. 1994, Nakagawa et al. 1998). The [C II] line is the dominant cooling line of the interstellar gas with an observed luminosity for the entire Milky Way of 5×10^{7} $L_\odot$ (see also Figure 4). The [C II]/FIR ratio is typically $\sim 3\times10^{-3}$. The [C II] emission from local H I clouds has been measured using small sounding rockets to be $\sim 3\times10^{-26}$ erg s^{-1} H–atom^{-1} (Bock et al. 1993). Independent estimates of the [C II] emission have been obtained using Copernicus, IUE and HST by measuring ultraviolet absorption lines originating from the upper level of this transition and these arrive at substantially the same value (Pottasch et al. 1979, Gry et al. 1992, Black 1993, using HST data from Cardelli et al. 1993).

The origin of this [C II] emission has been somewhat controversial (cf., Tielens 1995, 1997). Locally, the [C II] emission is dominated by emission from diffuse H I clouds heated through the photoelectric effect. [C II] 158 μm is the principal cooling line, resulting in gas temperatures of $\sim$ 80 K. In these clouds, the [C II]/FIR ratio provides a direct measure of the photoelectric heating efficiency of the dust. Toward the inner Galaxy, where the pressures and densities are higher, a substantial fraction of the [C II] emission may originate from the warm ionized medium (Heiles 1994). Also, much of the H I here is associated with the surfaces of molecular clouds illuminated by the ambient radiation field and these so-called PDRs (see §3) can be important contributors to the [C II] emission as well (Stacey et al. 1985, Shibai et al. 1991).

3. Photodissociation Regions (PDRs)

Photodissociation Regions, also called Photon-Dominated Regions (PDRs), are regions where far-ultraviolet (FUV) photons (6–13 eV) dominate the heating of the gas as well as their chemical structure. PDRs can be molecular clouds located close to bright O or B stars, neutral material at the edge of an H II region, reflection nebulae, dark-cloud edges, post-AGB stars and planetary nebulae. The diffuse clouds discussed above are low-density ($n < 1000$ cm^{-3}), low incident radiation field (less than 100 times the average interstellar field) versions of PDRs. Indeed, much of the neutral gas in the Galaxy is in the form of PDRs, as is the ISM in external galaxies. Figure 9 shows the IRAS image of molecular clouds in the Orion-Monoceros region. While some of the hot spots trace embedded massive YSOs, much of the diffuse emission is due to the conversion of FUV photons from the ambient O and B stars to infrared photons by the dust in the PDR surfaces.

The study of PDRs was triggered by the early observations of strong fine structure lines of [C II] 158 μm, [O I] 63 and 145 μm and [C I] 610 μm from dense molecular clouds in regions with nearby O stars (Melnick

PUT FIGURE 8 HERE

Figure 8. *Top: Far infrared [C* II*] 158 μm line intensity map of the galactic plane obtained by the BICE balloon. The intensity scales runs from 0 (purple)–6 (red)* $\times 10^{-4}$ *erg* s^{-1} cm^{-2} sr^{-1}*. Middle: Far infrared continuum map obtained from IRAS 60 and 100* μm *maps. The intensity scale runs from 0 (purple)–0.3 (red) erg* s^{-1} cm^{-2} sr^{-1}*. Bottom: The ratio of the far infrared [C* II*] line emission to the far infrared continuum emission. The scale runs from 0.0 (purple)–1.0 (red) %. The spatial resolution is about* $15'$ *(Nakagawa et al. 1998).*

et al. 1979, Storey et al. 1979, Phillips et al. 1980, Russell et al. 1980, Stacey et al. 1983). These lines were readily observable with the Lear Jet and KAO, and the data provided more accurate wavelengths than available from laboratory spectroscopy. The strong lines found in the Orion star-forming region stimulated the development of detailed physical and chemical models of PDRs (Tielens & Hollenbach 1985a,b). In addition, the discovery of strong and broad Unidentified InfraRed (UIR) features at mid-infrared wavelengths from the ground and the KAO in the same regions led to the study of PAHs. Together with the wealth of new ISO data, this field

PUT Figure 9 HERE

Figure 9. False color IRAS composite 12 (blue), 60 (green) , and 100 (red) μm image of the Orion constellation, covering a region of 30×24 degrees. The bright spot in the bottom part of this image is the sword region of Orion with the great nebula, M 42. The upper part of the figure is dominated by the ring–like shell surrounding λ–Orionis. The blue-ish dot to the left of this structure is the supergiant, Betelgeuse, one of the prominent stars in the Orion constellation. The other stars are not very bright in the infrared (Figure by D. Kester, personal communication).

has reached a significant level of maturity in a short time, and has provided important insights in the basic physics and chemistry of interstellar gas and dust irradiated by FUV photons. Comprehensive reviews have been given by Hollenbach & Tielens (1997, 1999).

3.1. PDRS: GAS PHASE

The structure of PDRs results from the interaction of FUV photons with the gas and dust through photoionization of atoms (i.p. C), photodissociation of molecules (i.p. H_2 and CO) and the photoelectric effect on grains. Models have been developed by various groups, with the most recent calculations presented by Kaufman et al. (1999). They generally consist of a plane parallel slab with a constant density $n_{\rm H}$ illuminated from one side by an intense radiation field, characterised by an enhancement factor G_o

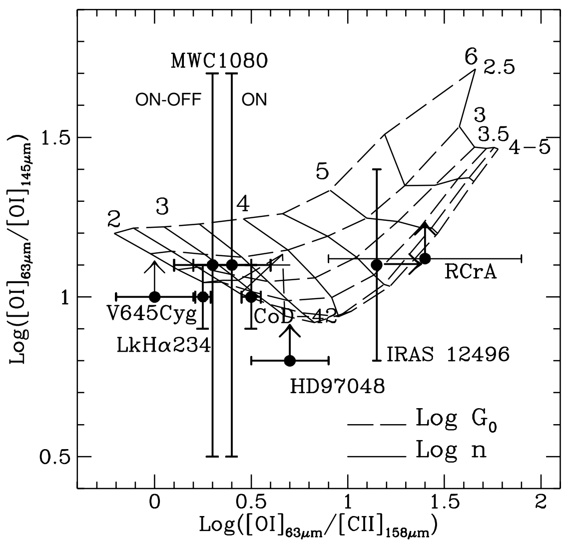

Figure 10. Line ratios of the principal fine-structure lines obtained in PDR models for different density n and radiation field G_o. The observed ratios with the ISO-LWS toward Herbig Ae stars are indicated (Lorenzetti et al. 1999).

over the average interstellar radiation field. At the edge, most of the gas is in atomic form, but at an attenuation in the visible of $A_V \approx 1-2$ mag, photodissociation of H_2 is decreased due to self-shielding and the transition from H to H_2 occurs. Deeper into the cloud, at $A_V \approx 2-4$ mag, the carbon balance shifts from C^+ to C and eventually CO (van Dishoeck & Black 1988). The oxygen not locked up in CO remains in atomic form up to $A_V \approx 8$ mag. The gas temperature is high at the edge ranging from 100 to 1000 K, but drops to less than 20 K deep inside the cloud. Typically, about 0.5% of the far-ultraviolet energy is converted into heating of the gas by the photoelectric effect, whereas the rest is absorbed and re-radiated as far-infrared dust continuum emission.

The high gas temperature at the edge results in bright atomic fine-structure lines of [C II], [O I], [C I] and [Si II] at mid- and far-infrared wavelengths. Since the critical densities and excitation temperatures of the lines span a range of values (10^3–3×10^5 cm^{-3}, 20–300 K), the observed line ratios are valuable probes of physical parameters, in particular the hydrogen density $n_{\rm H}$ and the enhancement of the radiation field G_o, which controls the temperature. Figure 10 illustrates how these lines can be used to constrain the PDR environment.

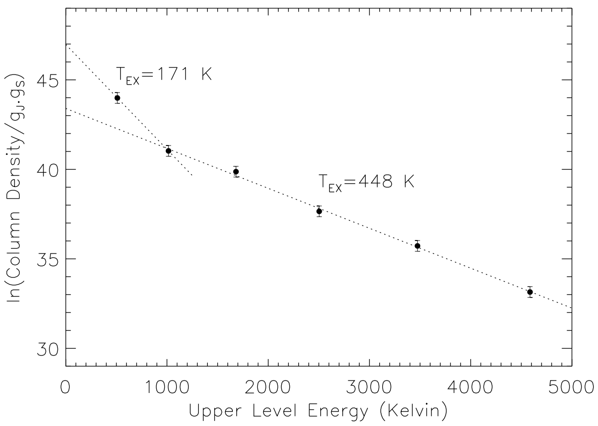

Figure 11. Rotational excitation diagram of H_2 for the PDR IC 1396 based on ISO-SWS observations. The different excitation temperatures derived from the J=2–3 and 3–7 levels indicate the presence of a temperature gradient through the region (Wright 2000).

The PDR interpretation was quickly accepted by the community, but a significant discussion arose from the fact that the observed lines persist deeper into the clouds than predicted by homogeneous models (e.g., Keene et al. 1985, Jaffe et al. 1987, Stutzki et al. 1988, Stacey et al. 1993). Many alternative models were developed, including dynamical cycling of the gas (Boland & de Jong 1983, Xie et al. 1995) and bistabilities in the chemical networks (Le Bourlot et al. 1995).The favored explanation is that the dense ISM is far from homogenous, but contains a 'clumpy' structure with a density contrast between the phases of at least a factor of 10.

A new probe of PDRs is provided by the pure-rotational lines of H_2 at 28 μm (J=2$\rightarrow$0), 17 μm (J=3$\rightarrow$1), 12μm (J=4$\rightarrow$2), etc. The 12 μm line was first detected by Beck et al. (1979), while the longer wavelength 17 μm line was observed by John Lacy and co-workers (Parmar et al. 1991). The ISO-SWS has allowed detection of the fundamental 28 μm line and routine observations of this and other lines in many regions (e.g., Timmermann et al. 1996, Thi et al. 1997, Draine & Bertoldi 1999, Fuente et al. 1999, see review by Wright 2000). Published results have been limited mostly to PDRs with strong H_2 lines, corresponding to regions with densities $n_{\rm H} > 10^4$ cm^{-3} and radiation fields $G_o > 100$ such as bright reflection nebulae. Maps of the higher-J lines at arcsec resolution have been made with ISO-CAM (e.g., Cesarsky et al. 2000). The rotational temperatures of $\sim 100 - 500$ K indicated by the J=2–7 lines directly reflect the kinetic temperature structure of the gas, since the lower rotational lines are populated primarily by collisions. The high vibrational temperature of $\sim$ 2000 K indicated by

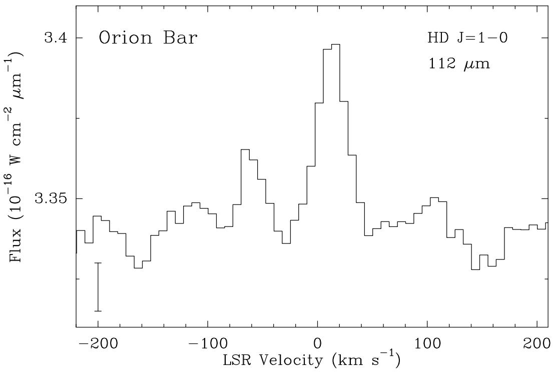

Figure 12. *Detection of the HD J=1–0 line at 112 μm with the ISO-LWS Fabry-Perot toward the Orion Bar. Together with observations of the H_2 pure rotational lines at 28 and 17 μm with the ISO-SWS, these data have been used to infer the [D]/[H] abundance ratio in an active star-forming region (Wright et al. 1999).*

ISO and ground-based 2 μm observations is due to ultraviolet pumping of the excited states (e.g., Black & van Dishoeck 1987, Sternberg & Dalgarno 1989). Existing PDR models give temperatures which are lower at the edge of the cloud than inferred from the ISO H_2 data, suggesting that either the photoelectric yield at the cloud edge is underestimated or that the H_2 formation occurs more rapidly than previously thought on high-temperature grains. While this uncertainty currently limits the astrophysical interpretation, it provides an instructive example of how astrophysical data can put constraints on basic chemical and physical processes which are difficult to study in a laboratory on Earth.

Another exciting new result is provided by the first detection of emission from the HD molecule in the ISM (Figure 12). HD is the main reservoir of deuterium in molecular clouds and can thus be used to constrain the primordial deuterium abundance produced by the Big Bang and its subsequent destruction in stars. Wright et al. (1999) detected the lowest rotational J=1$\rightarrow$0 line at 112 μm in the Orion Bar PDR with the ISO-LWS, whereas Bertoldi et al. (1999) observed the J=6$\rightarrow$5 line at 19.4 μm in the Orion shock with the ISO-SWS. Together with the H_2 pure rotational lines, the data give [D]/[H]=$(1.0 \pm 0.3) \times 10^{-5}$ and $(0.51 \pm 0.15) \times 10^{-5}$, respectively, significantly lower than the value of $(1.5 \pm 0.1) \times 10^{-5}$ inferred for the local ISM by Linsky (1996) from ultraviolet absorption line observations. This suggests destruction of deuterium in this active star-forming region.

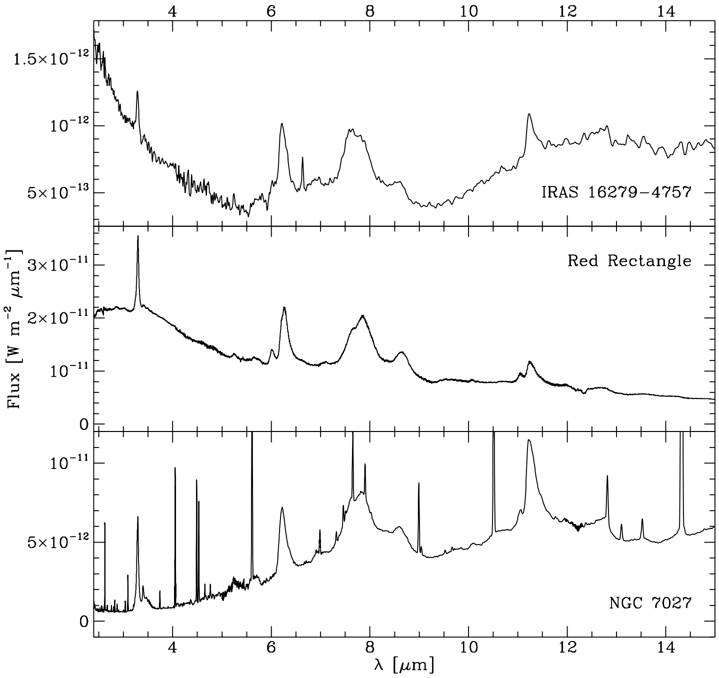

Figure 13. *The 3–15 μm emission spectra of the post–AGB objects, IRAS 16279-4757 and the Red Rectangle, and the planetary nebula NGC 7027, illustrating the rich and variable circumstellar PAH spectrum (Hony et al. 2000).*

3.2. INTERSTELLAR PAHS

Bright emission features at 3.3, 6.2, 7.7, 8.6, 11.3 μm, and a host of weaker ones dominate the mid–infrared spectra of many PDRs. Initially these bands were called the UIR features, and one of the first proposed identifications was carbonates, which have a band at 11.3 μm which matched the observed feature rather well (Gillett et al. 1973). This interpretation was supported by the presence of carbonates in meteorites, although it was difficult to envision an interaction between rock, CO_2 and liquid water in an interstellar setting. In any case, this interpretation formed the basis for extensive searches of the 5-8 μm region for the much stronger 6.8 μm carbonate band using the KAO (Russell et al. 1977, Willner et al. 1977). The interstellar spectra in this wavelength region are actually dominated by strong bands at 6.2 and 7.7 μm features and the carbonate suggestion died a quick death. Around the same time, a model was proposed based upon infrared fluorescence of simple molecules in an icy grain mantle (Allamandola & Norman 1978), but it was unclear how such simple ices could survive in the harsh FUV light of PDRs. Moreover, the composition of the mixture had to be tailored considerably. In retrospect, it is astonishing that it took almost 10 years to realize that the observed interstellar spectrum is that of Polycyclic Aromatic Hydrocarbon (PAH) compounds (Duley & Williams 1981), but it is now well accepted that the UIR bands are carried by such materials (see Léger & Puget 1984, Allamandola et al. 1985, Omont 1986 for early discussions, and Tielens et al. 1999, 2000 for recent reviews). The features are bright even far from the illuminating stars; hence, the emission has a non–thermal nature where the absorption of a single FUV photon raises the temperature of a small carrier to some 1000 K and this species cools through the emission in its vibrational modes (the UIR bands) (see §2.1). It is more appropriate to describe the carrier as a large molecule rather than a very small grain: borrowing molecular physicists' terminology, the process involves ultraviolet absorption into excited electronic states, which subsequently decay to lower states through a non-radiative process called internal conversion followed by vibrational emission. The observed color temperature corresponds to species containing about 50 C–atoms absorbing a $\sim$10 eV photon. Thus, the emitters are PAH molecules with about 50 C–atoms such as hexabenzocoronene ($C_{48}H_{24}$) and circumcoronene ($C_{54}H_{18}$). The PAHs also play a significant role in the energy balance, since the excess energy of the electrons produced by photoionization heats the gas (e.g., d'Hendecourt & Léger 1987, Bakes & Tielens 1994).

The ISO-SWS spectra of bright sources have revealed the incredible richness of the interstellar and circumstellar UIR spectrum. As an example, Figure 13 shows three spectra of C–rich post–AGB objects and planetary nebulae (Hony et al. 2000). Besides the well-known bands mentioned above, there is a wealth of weaker features: 3.4, 5.25, 5.65, 6.9, 10.5, 12.7 μm to mention some of them (Figure 13, Figure 14). Moreover, many of the prominent bands show satellite bands (e.g., 6.0, 11.0 μm) or break up into subfeatures (e.g., 7.6 and 7.8 μm).

One important characteristic of the UIR spectrum is its spectral variation. All sources show the five well–known UIR bands but their ratios can vary substantially and the 11.3/7.7 ratio in Figure 13 provides a good example. More dramatically, some H II regions show a 8.6 μm feature which dwarfs the commonly much brighter 7.7 μm feature (Roelfsema et al. 1996, Verstraete et al. 1996). More subtle variations are provided by the ratio of the 7.6/7.8 components of the 7.7 μm feature among H II regions and planetary nebulae. Also, often the features vary relative to each other with distance from the illuminating star within a single object (Geballe et al. 1989, Joblin et al. 1996, 2000). These variations make each spectrum unique and imply that the carriers are sensitive to the local physical conditions. It is quite clear from the data amassed that the UIR bands are carried by

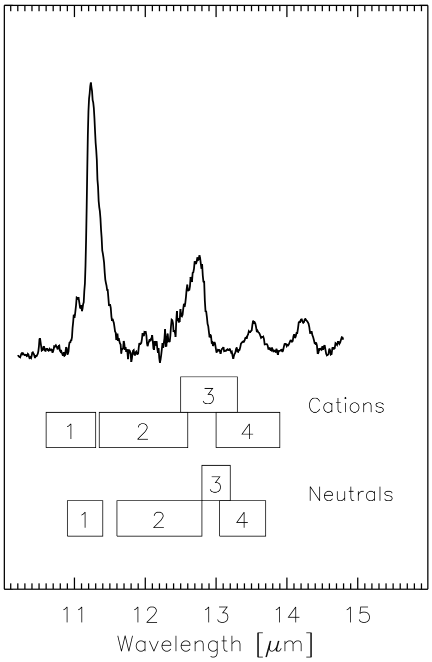

Figure 14. *The 10–15 μm spectrum of the Red Rectangle observed with the ISO-SWS, revealing new weak PAH bands (Hony et al. 2000). Bands in this spectral region are largely due to the C–H out-of-plane bending mode whose exact peak position is sensitive to the number of adjacent H–atoms involved. The boxes underneath the spectra give the ranges where neutral and cationic PAHs with the indicated number of adjacent H–atoms emit (Hudgins & Allamandola 1999). The band at 14.2 μm is attributed to C-C-C bending modes associated with PAHs having 3 or 5 adjacent H's.*

a family of related aromatic hydrocarbon compounds. Through correlation studies, the observed spectral variations carry the promise of actual identification of the specific molecular carriers involved. The enormous efforts in laboratory spectroscopy of PAHs (Hudgins & Allamandola 1999, 2000; Szczepanski & Vala 1993) supported by theoretical quantum chemical calculations (Langhoff 1996, Bauschlicher 1998) are essential for this purpose.

The 11–15 μm spectral region is characteristic for the C–H out-of-plane deformation mode and, therefore, for the edge structure of the emitting aromatic species (e.g., Duley & Williams 1981, Allamandola et al. 1989) (Figure 14). Due to coupling between the vibrating H–atoms, the exact peak position of these modes depends on the number of directly adjacent H–atoms (i.e., bonded to neighboring C atoms on a ring). Ionization shifts these ranges for the different number of adjacent H's to shorter wavelengths. The spectrum of the Red Rectangle, a post-AGB star, is shown in Figure

14 suggests a mix of neutral and ionized PAHs, with the strongest bands due to the “1” mode, but with “2” to “4” modes present as well (Hony et al. 2000).

Finally, an emission plateau in the 15–20 μm region has been discovered in the spectra of two intermediate mass young stars, so-called Herbig AeBe stars (van Kerckhoven et al. 2000). The dust continuum emission in the spectra of these stars starts at longer wavelengths than in most other sources and, hence, these weak features in the 15–20 μm region are more readily recognized here. However, this plateau is present in a variety of objects whose spectra are characterized by the UIR bands. Some spectra show a distinct feature at 16.4 μm superposed on this plateau (see also Moutou et al. 2000). These longer wavelength modes have been studied in the laboratory by Moutou et al. (1996) and Hudgins & Allamandola (2000). The emission is due to C–C–C bending modes which cause in-plane and out-of-plane distortions of the C–skeleton, and which are more molecule specific than the shorter wavelength bands. A collection of molecules gives rise then, in a natural way, to a plateau of blended emission features. Spectral substructure, in particular the 16.4 μm band, is likely characteristic for the smaller PAHs in the interstellar PAH family and may signal the presence of a pendant hexagonal ring. In general, this wavelength region has great potential for the identification of molecular structures which dominate the interstellar PAH family.

4. Shocks

Energetic input to the ISM is provided not only by ultraviolet photons but also by shocks, which are ubiquitous in the ISM. Shocks can be caused by many astrophysical phenomena, including supernova remnants interacting with the ISM, expanding H II regions, outflows from young stars, cloud-cloud collisions, and accretion onto circumstellar disks. General reviews of shocks have been given by Draine & McKee (1993) and Hollenbach (1997). For fast ($> 50 - 100$ km s^{-1}) shocks interacting with low-density material, the temperature is raised to very high values ($> 10^5$ K) instantaneously and most of the emission appears in atomic lines at ultraviolet wavelengths. These so-called “jump” or J-type shocks dissociate molecules within and ahead of the shock, and the molecules reform only slowly in a lengthy warm zone in the wake of the shock. For slower shocks impacting dense molecular clouds with a low ionization fraction, the hydrodynamical variables change more continuously and the temperatures in these C-type shocks reach peak values of only 2000–3000 K. The emission occurs primarily at infrared wavelengths in atomic fine-structure and molecular lines from H_2, CO, OH and H_2O. The diagnostic value of these lines has been elab-

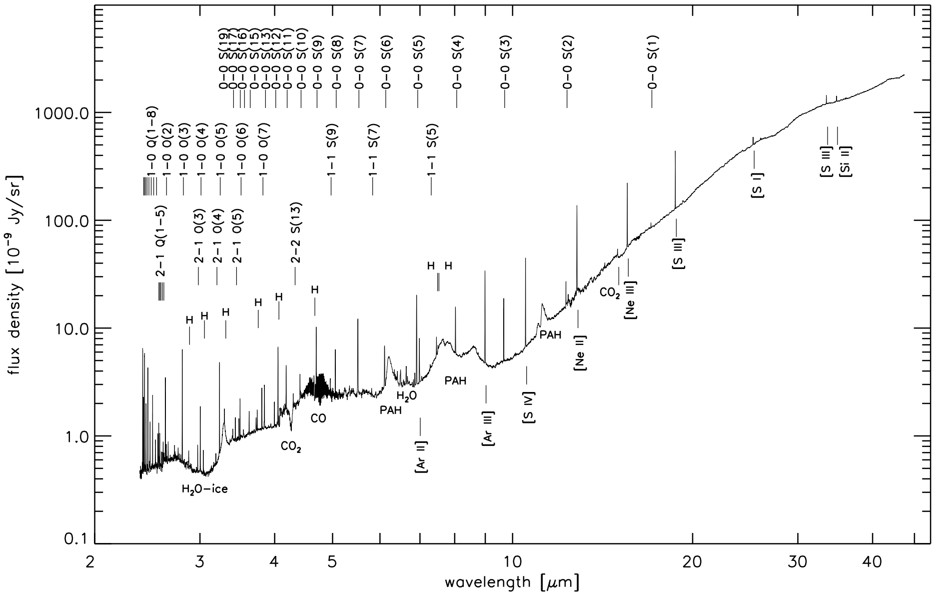

Figure 15. ISO-SWS grating scan of the Orion Peak 1 shock, showing a rich forest of H_2 lines and other features (Rosenthal et al. 2000).

orated by Hollenbach et al. (1989) and Kaufman & Neufeld (1996). Grain cores and mantles are also affected by shocks. In particular, high-velocity *J*-shocks cause disruption (through shattering) or non–thermal sputtering of the cores, resulting in much enhanced abundances of atomic Si, Mg, Fe, Ti, and Ca in the warm neutral phase of the ISM (Jones et al. 1996).

The best studied shock in the Galaxy is that associated with the Orion high-velocity outflow. Early KAO observations by several groups (e.g., Stacey et al. 1982, Watson et al. 1985, Melnick et al. 1987, Haas et al. 1991) revealed very strong, broad lines of CO high-*J*, [S I] 25 μm, OH 119 and 163 μm and other species, providing first tests of the model predictions. The subsequent ISO-SWS and LWS data centered at the shock "peak 1" region (see notation Beckwith et al. 1978) beautifully illustrate the rich infrared line spectrum (Figure 15, Bertoldi et al. 1999, Rosenthal et al. 2000, Cernicharo et al. 1999). The 2–20 μm region is dominated by a wealth of H_2 lines, which constrain the temperature structure in the shock. The data of Orion and other sources require at least two components with excitation temperatures between ~700 K and ~2000 K, respectively. Comparison with the models by Kaufman & Neufeld (1996) suggests a mixture of slow- and fast *C*-shocks, and perhaps a *J*-shock as well (see Wright 2000 for an overview). Such a mixture of shocks could reflect the fast direct impact and the slower oblique shocks expected for outflows. However, the high population of the J=27 level (which lies 42,500 K above the ground level) as derived from the observed S(25) line toward Orion is still a mystery and suggests that the basic physical structure of shocks is not yet fully understood.

ISOCAM–CVF maps of the higher-J lines at arcsec resolution have been presented by Cabrit et al. (1999) for young stellar objects and by Cesarsky et al. (1999) for the supernova remnant IC 443 interacting with the molecular cloud. No continuum emission is found in the latter object, but all of the broad-band IRAS 12 and 25 μm emission originally ascribed to warm dust is found to come from pure rotational H_2 line emission. Similarly, the IRAS 60 μm band may be dominated by the strong [O I] 63 μm line, emphasizing the importance of spectroscopy for the interpretation of broad-band colors. In general, the [C II] 158 μm/[O I] 63 μm and [O I] 63 μm/145 μm line ratios can be used to distinguish between low-velocity C- and high-velocity J-type shocks, but they often indicate a mix of shock types, like the H_2 lines. The [S I] 25 μm is an excellent diagnostic of shocks vs. PDRs.

The power of heterodyne instruments in space is illustrated by spectrally-resolved observations of [C II] and [O I] profiles, as well as high-J lines of OH and CO and their isotopes (Boreiko & Betz 1996a,b; Betz & Boreiko 1989; Keene et al. 1998, 1999), and HCl (Blake et al. 1985). These data provide important constraints on the different interpretations, especially in distinguishing shocks and PDRs.

The H_2O molecule is a particularly powerful probe of C-type shocks. H_2O is predicted to be the dominant oxygen-bearing species in warm, dense gas, because most of the available oxygen is driven into H_2O at high temperatures (T >230 K) through the reactions O + H_2 $\rightarrow$ OH + H and OH + H_2 $\rightarrow$ H_2O + H increasing its abundance by orders of magnitude (e.g., Neufeld & Melnick 1987, Ceccarelli et al. 1996, Charnley 1997). In addition, the H_2O level populations are sensitive to collisions and to pumping by far-infrared radiation due to warm dust. Finally, H_2O contributes to the cooling and heating of the gas (e.g., Neufeld & Kaufman 1993). Pioneering airborne observations of $H_2{}^{18}O$ by Zmuidzinas et al. (1995) indicate that the H_2O abundance is low, $< 10^{-7}$, in quiescent clouds, but early observations of masing lines from the KAO and ground hinted already at enhanced abundances up to $10^{-5} - 10^{-4}$ in warm shocked gas (e.g., Waters et al. 1979, Phillips et al. 1980, Melnick et al. 1993, Cernicharo et al. 1994). Ground-based and airborne observations of H_2O are greatly hampered by the Earth's atmosphere, however, and the derivation of abundances from masing lines is tricky. ISO has provided the first opportunity to observe a large variety of non-masing H_2O lines in YSOs, including both lower and higher excitation lines. Figure 16 shows a sample of the wealth of pure ro-

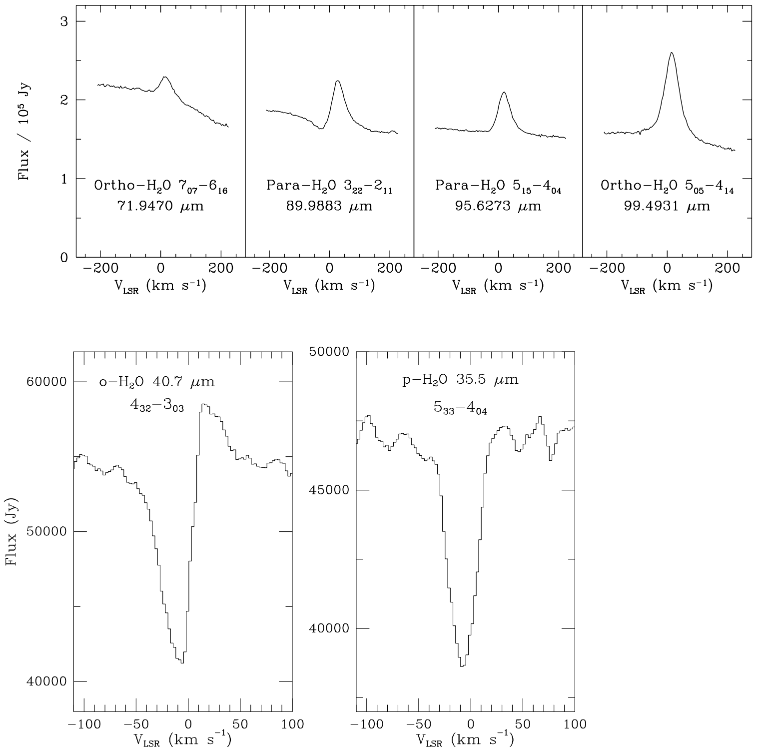

Figure 16. Examples of high-J emission and absorption lines of H_2O for the Orion shock observed with the ISO-LWS (top) and SWS (bottom) Fabry-Perot, revealing broad and complex line profiles and high abundances (Harwit et al. 1998, Wright et al. 2000).

tational H_2O lines detected with ISO toward the Orion shock (Harwit et al. 1998, Cernicharo et al. 1999, Wright et al. 2000). The main conclusion from these data is that the H_2O abundance is indeed high in warm regions and rises up to a few $\times 10^{-4}$ with respect to H_2 in the case of Orion, locking up a significant fraction of the available gas-phase oxygen.

The recent launch of the SWAS satellite allows observations of spectrally resolved profiles of the lowest ortho-H_2O $1_{10} - 1_{01}$ transition at 538 μm above the Earth's atmosphere (Melnick 2000, Melnick et al. 2000, Figure 17). This line can be used to probe the H_2O abundance not only in warm clouds but also in cold gas to which ISO was insensitive. The first results indicate that the H_2O abundance is even lower than indicated before ($\lesssim 10^{-8}$) in quiescent clouds. Moreover, O_2 has a surprisingly low abundance in molecular clouds, as indicated by SWAS and balloon-borne observations (Olofsson et al. 1998, Goldsmith et al. 2000). Future obser-

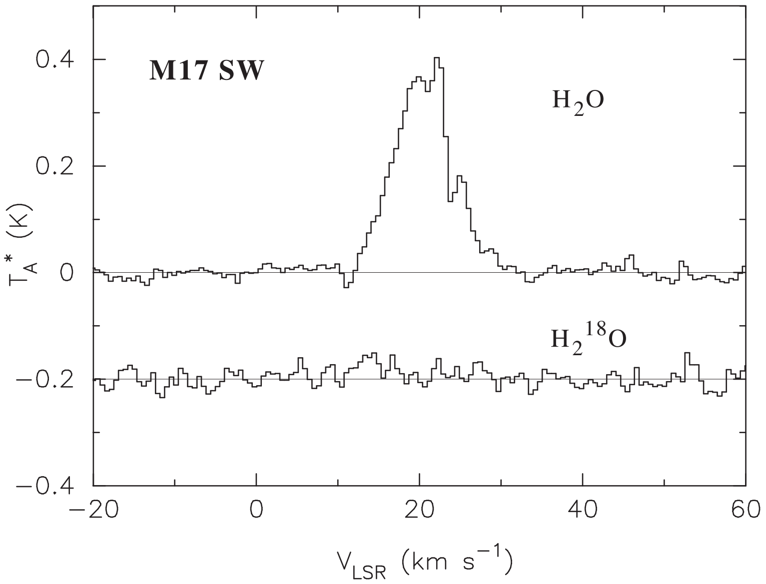

Figure 17. *SWAS observations of the $1_{10} - 1_{01}$ ortho-H_2O and $H_2^{18}O$ ground-state line toward the M 17 star-forming region (Melnick 2000, Snell et al. 2000).*

vations with the Sweden-France-Canada ODIN satellite will allow deeper searches for O_2. The low H_2O and O_2 abundances can be explained by enhanced photodissociation in extended low-density inhomogeneous clouds (Spaans & van Dishoeck 2001) and freeze-out of oxygen in cold dense clouds (Bergin et al. 2000).

5. Cold envelopes around YSOs: Ices

The gas and dust in the cold outer envelopes around young stellar objects (YSOs) are best probed through infrared absorption lines toward embedded sources. The young stars heat the dust in their immediate surroundings to a few hundred K, providing a continuum against which the cooler foreground species can be seen in absorption (cf. §2.2). The quiescent medium can also be studied by this technique, if a bright infrared background star can be found. Such observations provide a powerful complement to submillimeter emission line studies: only a pencil beam toward the source is probed in absorption, and both the gas and the dust can be observed along the same line-of-sight.

Since the densities are high and the temperatures low, the timescales for gas-phase atoms and molecules to collide with the cold ($\sim$ 10 K) grains and stick are short, less than 10^5 yr. Thus, most gas-phase species are expected

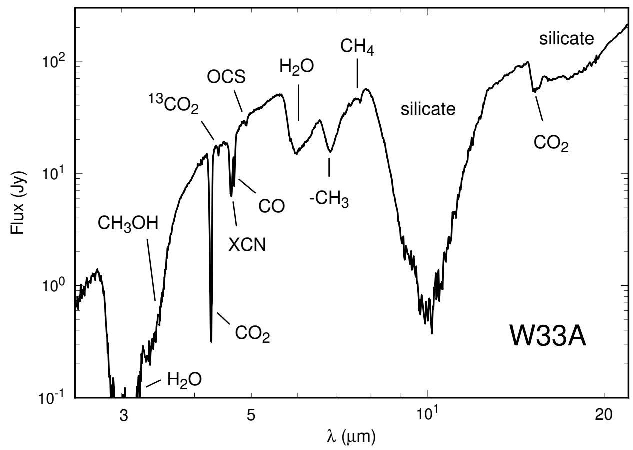

Figure 18. *The 2.5–25 μm spectrum of embedded massive protostar W 33A obtained with the ISO-SWS at a resolving power of 500–1000. Except for the 10 μm silicate band, all features are due to simple molecules in ice mantles (Gibb et al. 2000).*

to freeze-out onto the grain cores and form an icy mantle. While H_2O ice was ruled out as an important dust component in the diffuse ISM by ground–based observations (Gillett et al. 1975), H_2O-ice was discovered in the shielded environment of dense interstellar clouds in the 1970's (Gillett & Forrest 1973). The study of ices was subsequently pursued from ground and airborne platforms (e.g., Willner et al. 1982, Tielens et al. 1991). However, even from the KAO important regions of the spectrum around 4.2 and 15 μm were inaccessible due to telluric CO_2. The large and systematic database obtained with the ISO-SWS provided the first complete, unbiased census and is particularly suitable to study the composition and evolution of interstellar ices. Recent reviews are given by Tielens & Whittet (1997), d'Hendecourt et al. (1999) and Ehrenfreund & Schutte (2000).

Infrared spectra of YSOs such as the massive protostar W 33A (Figure 18, Gibb et al. 2000) show a variety of solid state absorption features due to simple molecules in an icy mixture. Such ices are a major component of interstellar dust inside dense clouds locking up a substantial fraction of the available elements, in abundances quite comparable to gaseous CO. These ices are formed by accretion and reaction on the pre-existing grain cores and their composition allows a direct probe of grain surface chemistry (Tielens & Hagen 1982). In the hot cores around luminous protostars, evaporation of the ices drives a rich and complex chemistry mainly through the release of copious amounts of CH_3OH into the gas phase (see §6). Finally, agglomeration of interstellar ice grains in the outer regions of the solar nebula is thought to be the first step in the formation of comets, icy satellites, and planets. Similar processes may play a role in the circumstellar disks around protostars (§7).

The spectrum of W 33A shows the spectral signature of H_2O ice (3 bands), CO_2 ice (3 bands), and solid CO, OCS, CH_4, and CH_3OH (1 band, each) (for a critical discussion of these assignments see Tielens & Whittet 1997 and Ehrenfreund & Schutte 2000). The identification of the bands at 4.62 and 6.85 μm is still somewhat controversial, although a strong case for the identification of the 4.62 μm feature with OCN^- has been made (Schutte & Greenberg 1997, Demyk et al. 1998, Palumbo et al. 2000). Extensive laboratory studies by various groups have been essential in the analysis of these data. While previous low–resolution, ground–based and airborne observations had revealed tantalizing hints of the presence of solid CO_2 and CH_4 (d'Hendecourt & de Muizon 1989, Lacy et al. 1991, Boogert et al. 1997), the ISO-SWS allowed for the first time a detailed study of these ice compounds and allowed their potential as diagnostic probes of the environment to be fully developed. Some illustrative examples are discussed below.

5.1. THERMAL PROCESSING AND ICE SEGREGATION

Solid CO_2 is an important component of interstellar ices in star-forming regions as evidenced by its strong stretching and bending modes (see Figure 18; de Graauw et al. 1996, d'Hendecourt et al. 1996, Gerakines et al. 1999). All of these bands show variations in peak position and profile from source to source due to different structures of the ice (Figure 19). The CO_2 bending mode at 15 μm is an especially sensitive diagnostic of the CO_2 ice environment and the degree of thermal processing by the nearby protostar. Extensive laboratory studies on a variety of astrophysically relevant mixtures at the Leiden laboratory have shown that these variations are due to thermal processing of ice mixtures containing CO_2, H_2O, and CH_3OH in a ratio of approximately 1:1:1 (Ehrenfreund et al. 1998, 1999). The triple structure in the spectra is formed when, upon heating to $\sim$ 100 K, the ice matrix rearranges and molecules start to be mobile within the ice matrix. The two narrow peaks are due to "pure" CO_2 clusters in a H_2O/CH_3OH ice environment. The shoulder at longer wavelengths is due to a complex between CO_2 and CH_3OH. The stretching mode of $^{13}CO_2$ ice at 4.38 μm (Figure 18) has also been detected in a large number of sources and a detailed analysis of its profile corroborates this conclusion (Boogert et al. 2000). These results provide important evidence for extensive ice segrega-

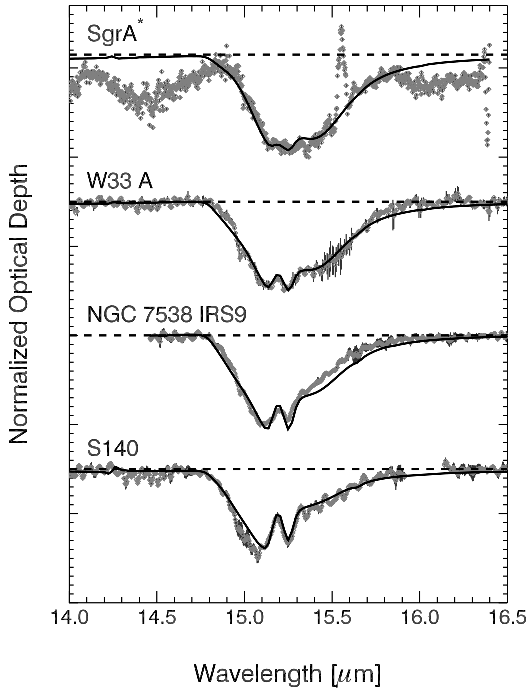

Figure 19. *ISO-SWS spectra of the CO_2 bending mode near 15 μm, illustrating the thermal evolution of interstellar ices. The sources are displayed in order of increasing gas temperature. Solid lines are fits based upon laboratory data for an ice mixture H_2O:CH_3OH:CO_2=1:1:1 at temperatures ranging from 106 to 118 K in the laboratory (corresponding to 50–60 K under interstellar conditions) (Gerakines et al. 1999).*

tion and thermal processing in the envelopes around massive protostars (see Figure 21).

One of the most prominent, but as yet unidentified, ice bands in the absorption spectra of protostars occurs at 6.85 μm (Schutte et al. 1996, Keane et al. 2000, Figure 20). Due to the limited resolution of earlier airborne observations the peak position of this feature was assumed to be constant at 6.85 μm (Tielens & Allamandola 1987b). However the new high resolution ISO-SWS observations show that the position varies considerably between the observed lines of sight in a systematic way similar to that found for solid CO_2. The observed profiles of all sources can be fitted with a combination of two extreme features, suggesting that they reflect different degrees of thermal processing toward these protostars. While the actual carrier of this band is currently unknown, this sensitivity to the physical characteristics of its (ice) environment provides additional constraints for the identification

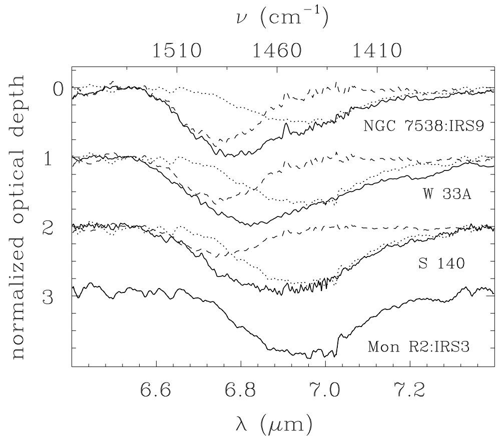

Figure 20. Observed ISO-SWS 6.8 μm band in the spectra of luminous protostars, on a normalized optical depth scale. All profiles can be fitted by combinations of two "extreme" profiles (dotted and dashed lines) whose relative strengths reflect the degree of thermal processing of the ice along the line of sight. Note that some profiles show narrow absorption lines due to warm, gaseous water vapor (Keane et al. 2000).

which will assist laboratory identification efforts.

5.2. GRAIN SURFACE CHEMISTRY: SOLID CH_4

A weak band at 7.6 μm in the spectra of some deeply embedded protostars has been attributed to CH_4 ice (Boogert et al. 1996, 1998) and it is of interest to compare its implications with those derived from the 4.67 μm solid CO band. Studies of the profile of the latter band have revealed that much of the solid CO is not mixed in with polar molecules (i.e., H_2O; Tielens et al. 1991, Chiar et al. 1998), implying that along most lines–of–sight there are, at least, two independent ice components: a water–rich ice dominating the bulk of the interstellar ice and a second ice component containing only non–polar molecules such as (most of) the solid CO. The presence of these two independent components may reflect thermal processing (see Figure 21) — the volatile CO is outgassed at much lower temperatures than H_2O — or differences in the chemical history between these two species — H_2O ice is formed on grain surfaces in the presence of atomic H which also reduces CO to H_2CO and CH_3OH. The importance of thermal processing of interstellar ices is attested for by the observed profiles of the solid CO_2 ice bands (§5.1). Solid CH_4 provides another good test for these different scenarios: solid CH_4 is as volatile as solid CO, but chemically, CH_4 is formed on grain surfaces through hydrogenation of accreted atomic C. The observed solid CH_4 band is well fitted by traces of CH_4 in polar, H_2O-rich ices rather than CO-rich ices (Boogert et al. 1996). Hence, for CH_4, chemistry seems to be more

TABLE 2. Observed interstellar and cometary ice composition[a]

Species	NGC 7538 IRS 9	W 33A	Hale–Bopp
H_2O	100	100	100
CO (total)	10	3	23
CO (polar)	3	2	
CO (apolar)	7	1	
CO_2	16	4	6
CO_2 (polar)	1	1	
CO_2 (annealed)	3	2	
CH_3OH	9	10	2
H_2CO	3	2	1
HCOOH	2	0.5	0.1
NH_3	10	4	0.7
CH_4	1	0.4	0.6
OCS	0.1	0.05	0.4
'XCN'	0.8	1	

[a] Relative to H_2O=100. Adopted H_2O column densities are 10^{19} and 4×10^{19} cm^{-2} for NGC 7538 IRS 9 and W 33A, respectively.
References: Interstellar ices: H_2O, H_2CO, HCOOH: Keane et al. (2000); CO: Tielens et al. (1991); CO_2: Gerakines et al. (1999); CH_3OH: Allamandola et al. (1992); NH_3: Lacy et al. (1998); CH_4: Boogert et al. (1998); OCS: Palumbo et al. (1997); 'XCN': Pendleton et al. (1999). Comet Hale Bopp: Bockelée-Morvan et al. (2000).

important in driving the ice environment than thermal processing.

5.3. THE INTERSTELLAR AND COMETARY ICE INVENTORY

Table 2 summarizes the observed composition of interstellar ice toward the massive protostars NGC 7538 IRS 9 and W 33A. H_2O dominates the column density of ice by a large factor. The carbon–bearing species CO, CO_2 and CH_3OH, are less abundant by a factor 10 to 100, while H_2CO, HCOOH, and CH_4 are at the 1% level compared to H_2O. This dominance of H_2O is directly evident from the complete infrared spectrum of this source (Figure 18). Possibly an exception should be made for the homonuclear molecules O_2 and N_2 which have no infrared active vibrational modes. While the solid matrix will perturb these modes into (very weak) activity, these bands are difficult to detect (Ehrenfreund et al. 1992, Vandenbussche et al. 1999).

This global ice inventory is somewhat misleading since, as emphasized above, analysis of the observed ice profiles have revealed the presence of a number of independent ice components along most lines of sight. These components likely reflect the effects of spatial variations in (1) the composition of the accreting gas which sets the stage for grain surface chemistry and (2) in segregation and outgassing of more volatile ice species driven by heating by the nearby YSO (see Figure 21).

The most striking aspect of the infrared spectrum is the apparent simplicity of the composition of interstellar ices. The molecules are highly hydrogenated but also show oxidation. Furthermore, the abundance of these species is much higher in the ice than in the gas phase of dark clouds. The H_2O/CO ratio is quite telling: less than 10^{-3} in the gas in dark clouds (Melnick 2000) compared to 10 in the ice. This preference for saturated species and this abundance difference implicates a chemical origin different from gas phase ion–molecule chemistry. Clearly, H_2O ice is a major reservoir of oxygen formed by hydrogenation of O and/or via O_2 (Tielens & Hagen 1982). Also, given the low abundances of solid NH_3 and CH_4, accretion on the grain mantle occurred from a molecular gas in which most of the nitrogen and carbon is locked up in N_2 and CO. Furthermore, hydrogenation of CO leads to the formation of the carbon species H_2CO, CH_3OH, and HCOOH while oxidation results in CO_2. Observations of the deuterated versions of these species in hot cores also support the dominance of reactions on grain surfaces (Tielens 1983, Turner 1990, Ceccarelli et al. 1998a). Finally, except for the 4.62 μm XCN band and the 6.85 μm band whose identifications are still somewhat controversial, no unidentified bands are present. Clearly, grain (surface) chemistry heavily favors simple species and, as a corrollary, the role of surface chemistry and UV photolysis in producing more complex molecules seems limited to abundances which are at least an order of magnitude lower.

Comets are generally thought to contain a rather pristine record of the interstellar cloud from which the Sun and its planetary system were formed. It is therefore of some interest to compare the interstellar ice abundances to those measured for comets. Table 2 compares observed ice compositions to those of comet Hale Bopp (Bockelée-Morvan et al. 2000). It should be understood that a wider array of species has been observed in comets, largely because near the Sun the ices evaporate and simple gaseous species are more readily observed through their rotational spectra at millimeter wavelengths. Nevertheless, the species dominating the infrared spectra of interstellar ices are also abundant in comets. Even their relative abundances are quite comparable (Table 2), lending credence to their evolutionary interrelationship. A "shared" chemical history is also supported by the high deuteration observed in cometary molecules (Irvine et al. 2000).

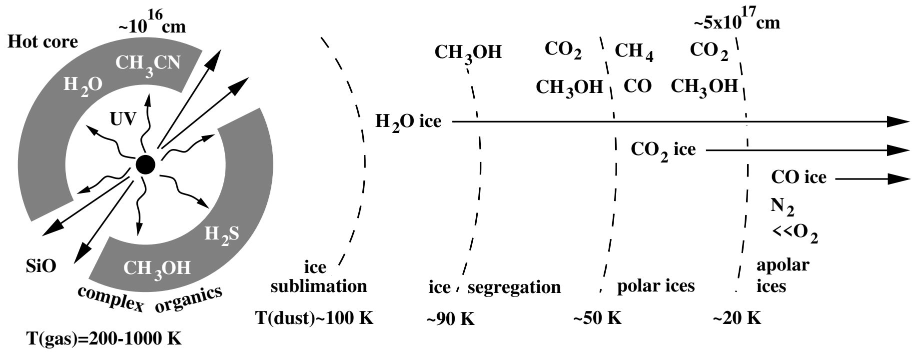

Figure 21. *Schematic illustration of the temperature structure of the envelopes of YSOs and the different ice phases due to heating and thermal desorption. In the inner hot core, the ices have evaporated and high-temperature 'hot core' chemistry occurs (van Dishoeck & Hogerheijde 1999).*

6. Warm inner envelopes around YSOs

Young stars heat their surrounding envelopes, resulting in a temperature gradient throughout the surrounding gas and dust (Figure 21). For a $\sim 10^5$ $L_\odot$ source like W 33A and Orion IRc2, the region where $T_{\rm dust} \approx T_{\rm gas} > 90$ K extends to $\sim 10^{16}$ cm ($\sim$ 1000 AU) from the star, whereas the region with $T_{\rm dust} > 20$ K extends to $\sim 5 \times 10^{17}$ cm (0.1 pc). All ices are evaporated in the inner part of the envelope above 90 K, i.e., within a few arcsec for a typical distance of 1 kpc. In this so-called "hot core" region, the released ices can drive a rich chemistry in the gas phase. Particularly, CH_3OH is a key ingredient in driving molecular complexity (Charnley et al. 1992, Caselli et al. 1993).

In addition to radiative heating, the interaction of the outflow from the young star with the envelope can result in enhanced temperatures. At the positions of direct impact, the temperature is raised to several thousand K or more, depending on the speed of the shock (see §4). Turbulent mixing along the outflow walls results in slow entrainment of the gas and dust with removal of the ice mantles. Finally, once young massive stars clear their surroundings, ultraviolet radiation creates a PDR at the surrounding cloud (see §3). The different diagnostic probes discussed in the preceeding sections can be used to disentangle their effects, to determine their relative importance and to establish an evolutionary sequence for the objects (van Dishoeck & van der Tak 2000, van den Ancker et al. 2000a).

The presence of warm gas along the line of sight toward protostars is clearly revealed in their absorption spectra, seen first in ground-based observations of gas-phase CO at 4.7 μm (Mitchell et al. 1990). The ISO-SWS

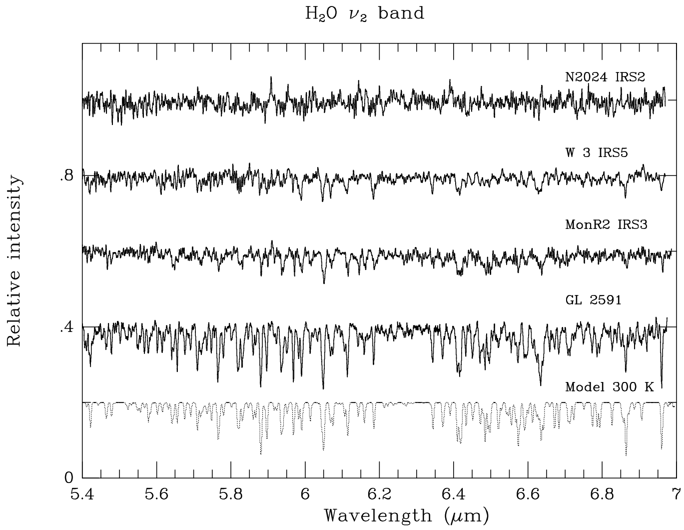

Figure 22. *Absorption by gas-phase H_2O in the ν_2 bending mode at 6 μm observed toward massive YSOs with the ISO-SWS (van Dishoeck & Helmich 1996, Boonman et al. 2000).*

has allowed searches for other gas-phase molecules, in particular H_2O and CO_2 which cannot be observed from the ground and which are among the dominant O- and C-containing species (see van Dishoeck et al. 1999 for review). One of the early SWS surprises included the detection of abundant ($\sim$few $\times 10^{-5}$ with respect to H_2), hot ($T_{\rm ex} \approx 300$ K) gas-phase H_2O absorption toward a number of YSOs (Helmich et al. 1996, van Dishoeck & Helmich 1996, van Dishoeck 1998) (Figure 22). In contrast, the abundance of gas-phase CO_2 was found to be much lower, a few $\times 10^{-7}$ (van Dishoeck et al. 1996, Dartois et al. 1998, Boonman et al. 2000). Gas-phase CH_4 (Boogert et al. 1998), C_2H_2 and HCN (Lacy et al. 1989, Evans et al. 1991, Lahuis & van Dishoeck 2000) have also been detected, with abundances up to 10^{-6} and high excitation temperatures.

The gas-phase results, combined with the solid-state data for the same lines of sight, allow the gas/solid ratios to be determined. Significant trends are found in increasing abundances of evaporated molecules and gas/solid ratios with increasing temperature for the different objects. These trends mirror those found for the fraction of heated ices from the solid CO_2 and 6.85 μm bands (Figure 19, Figure 20) (Boogert et al. 2000). Since these diverse phenomena involve a range of temperatures from < 100 K to 1000 K, the enhanced temperatures must be communicated to both the inner and

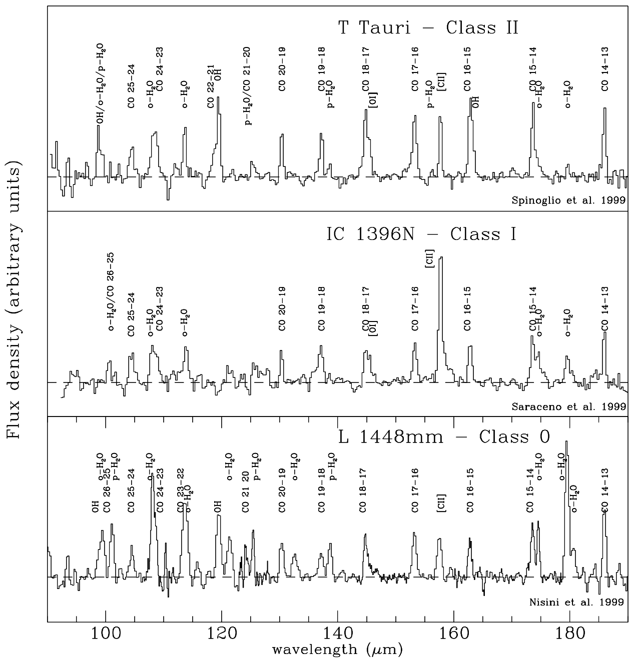

Figure 23. ISO-LWS spectra of low-mass young stellar objects at different stages of evolution, revealing a wealth of CO, OH and/or H_2O pure rotational lines. The continuum has been subtracted. Top: T Tauri (Spinoglio et al. 2000); Middle: IC 1396N (Saraceno et al. 1999); Bottom: L1448mm (Nisini et al. 1999).

outer parts of the envelopes. Van der Tak et al. (2000) show that this 'global heating' plausibly results from the gradual dispersion of the envelopes with time: the more evolved objects have removed a larger fraction of their envelope, resulting in a smaller ratio of envelope mass to stellar mass and thus a higher temperature throughout the envelope. Thus, these signatures can be used as a probe of the evolutionary state of the objects.

Emission line observations with the ISO-LWS are also a powerful tool to trace the warm gas surrounding YSOs, and to distinguish between the various mechanisms for heating and clearing of the envelope (see Saraceno et al. 1999 for an overview). The youngest, deeply embedded low-luminosity ($< 10^3$ $L_\odot$) sources, so-called "class 0" objects) have very rich LWS spectra with many molecular lines due to H_2O, OH and CO (e.g., Liseau et al. 1996, Ceccarelli et al. 1998b, Nisini et al. 1999, Spinoglio et al. 2000, see Figure 23). The CO excitation indicates high temperatures of a few hundred K and high densities over a region of a few arcsec (500–1000 AU) in size. In objects in later evolutionary stages (class I and II) the total luminosity in the CO lines, and thus the total cooling, is higher than that in the H_2O or OH lines. In contrast, high luminosity sources ($> 10^4$ L$_\odot$) show strong atomic and ionic lines, in particular [C II] 158 μm and [O I] 63 and 145 μm emission, with weaker molecular lines. The main exception is formed by Orion and by massive sources in the Galactic center region, which exhibit strong H_2O and OH emission and absorption lines (see §4, Baluteau et al. 1997). One possible explanation for this difference is that heating by radiation plays a larger role in the case of high-mass objects whereas heating by shocks is more important in the lower-mass case. Higher-mass objects are also more distant, so that the emission from warm molecular gas suffers more beam dilution.

An interesting case where both heating processes may contribute equally is formed by the intermediate mass Herbig Ae/Be stars. Van den Ancker et al. (2000a,b) have observed a large sample of these objects with the ISO-SWS, and used various diagnostics to distinguish the dominant excitation mechanism. In these mixed cases, the atomic and ionic lines provide good additional diagnostics. Specifically, the [Si II] 34.8 μm and [Fe II] 26.0 μm lines are strong in PDRs, whereas the [S I] 25.2 μm line becomes detectable only in shocks. The same trend is also found from ISO-LWS data of the [O I] 63 μm line: in low-luminosity YSOs the [O I] emission appears primarily due to shocks, whereas higher-mass Herbig Ae/Be objects have additional contributions from PDRs (cf. Figure 10, Lorenzetti et al. 1999, Giannini et al. 1999).

The evolutionary sequence of intermediate mass YSOs is beautifully illustrated by their complete mid-infrared spectra (Figure 24, van den Ancker et al. 2000a). The ISO-SWS spectrum of the very young, deeply embedded object LkHα 225 reveals a large column of solid water ice and silicates as well as absorption bands due to gas-phase H_2O, CO and CO_2. This spectrum also contains many emission lines due to molecular hydrogen, [S I], [Si II] and [Fe II], arising in shocks caused by the protostellar outflow driving into the surrounding material. LkHα 224 is slightly older and its spectrum does not show absorption features due to dust or gas anymore; much of the ice has evaporated and the envelope dispersed. The absence of dust emission features suggests that the spectrum is dominated by emission from very large grains ($\gg$ 10 μm). The spectrum of BD+40 4124, which has already cleared its environment, shows emission bands from PAHs, as well as emission lines from H I, H_2, [Fe II] and [Si II] characteristic of an H II region surrounded by a PDR. The Herbig Ae star AB Aur — a pre–main sequence star surrounded by a circumstellar disk and remnant envelope (see §7) — shows, like BD+40 4124, the characteristics of ionized gas and a PDR. However, the PAHs are less prominent in this source and silicate emission starts to dominate the mid–infrared dust features. The spectrum of HD

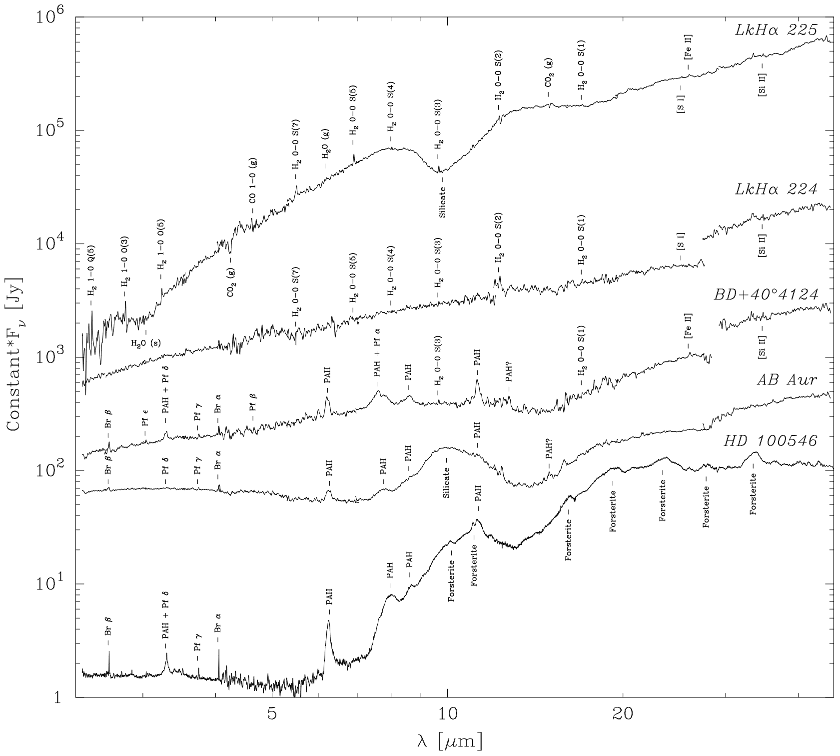

Figure 24. *The ISO-SWS mid–infrared spectra of newly-formed stars in different stages of formation (van den Ancker et al. 2000a,c; Malfait et al. 1998). From top to bottom – in a rough evolutionary sequence – the spectra change from dominated by solid state absorption features and gas (shock) emission lines, to featureless, to PAH features and PDR lines, to amorphous and then crystalline silicates with H* I *recombination lines.*

100546, an even more evolved member of this class, reveals the presence of a small fraction of cool crystalline silicates as well as weak PAH features. Except for the H I recombination lines, originating from the disk, all other spectral lines have disappeared in these latter phases. These spectral variations are related to the relatively rapid (10^6 yr) accretion and/or dispersion of the surrounding molecular cloud material and the slower ($\sim 10^7 - 10^8$ yr) processing of the dust (agglomeration, settling, and destruction) in the circumstellar disk.

7. Circumstellar disks around young stars

Circumstellar disks around young stars provide the raw material from which planetesimals and eventually planets may form, and are therefore popular targets for new high spatial resolution instrumentation. The presence of these disks was first inferred from ground-based observations at infrared and millimeter wavelengths (see Beckwith & Sargent 1996 for an overview), but they have also been revealed as silhouettes against bright backgrounds through stunning space-based HST images (e.g., McCaughrean & O'Dell 1996). The typical sizes of the disks are ∼100–400 AU, comparable to that of our own solar system. In order to study the composition and evolution of the dust and gas in such disks, spectroscopy at infrared wavelengths is essential. An overview is presented by Waelkens (this volume), but a few examples are included here to illustrate the cosmic dust cycle.

7.1. SOLID-STATE FEATURES

Early ground-based and airborne observations of solid-state features in disks have mostly been limited to the 10 μm silicate feature (e.g., Telesco & Knacke 1991, Sitko et al. 1999). This feature has also been observed for a sample of T Tauri stars with ISOPHOT-S (Meyer et al. 2000). The full richness of circumstellar disk spectra is only revealed through complete mid- and far-infrared spectroscopy as provided by the ISO-SWS and LWS. Because of the sensitivity of these instruments, the observations have been possible only for intermediate mass Herbig Ae stars, but not yet for solar-mass T Tauri stars. A striking example is presented by the case of HD 100546, a ∼10 Myr old Herbig Ae star, whose disk shows emission from PAHs and crystalline silicates, in particular forsterite (Mg_2SiO_4) (Waelkens et al. 1996, Malfait et al. 1998, Figure 27). The spectrum of the dust in this disk greatly resembles that of comet Hale-Bopp (Crovisier et al. 1997), suggesting some connection between interstellar and cometary material. In contrast, the dust around AB Aur is dominated by warm amorphous olivines and crystalline iron oxides, with PAH features detected. Crystalline H_2O ice is also detected in a few cases (van den Ancker et al. 2000b, Molinari et al. 1999). Thus, the dust spectral characteristics show evidence for significant processing in some sources, which may be partly due to age but which may also reflect local processes caused, for example, by the presence of nearby companions or the possible formation of planetary bodies.

7.2. GASEOUS SPECIES

A major question in the evolution of disks is the timescale over which the gas disappears from the disk, since this directly affects the formation of gaseous giant planets. Most studies of the gas have been based on ground-based millimeter observations of CO (e.g., Koerner & Sargent 1995, Zuckerman et al. 1995, Dutrey et al. 1996), but the analysis of these data suffers from optical depth effects in the lines and possible freeze-out of the molecules onto grains in the coldest regions. The lowest H_2 pure rotational lines provide a

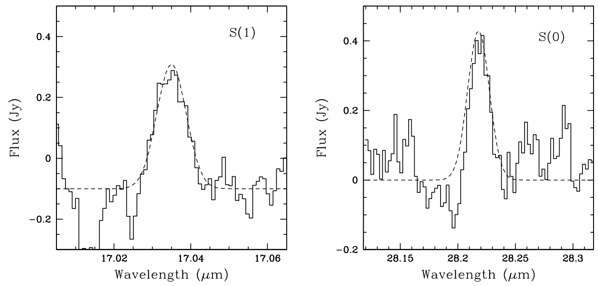

Figure 25. ISO–SWS spectra of the H_2 S(0) and S(1) lines toward the isolated T Tauri object GG Tau. This double-binary system is surrounded by a circumstellar dust and gas disk with a size of ∼800 AU. The H_2 lines provide direct information on the temperature and amount of warm gas (Thi et al. 1999a).

powerful complement to CO, since they directly measure the amount and temperature of the gas, provided it is warm enough to emit in these lines ($>$ 80 K).

Deep searches for the H_2 S(0) and S(1) lines at 28 and 17 μm have been performed with the ISO-SWS toward a dozen young stars with confirmed circumstellar disks (Thi et al. 1999a,b; Stapelfeldt et al. 1999, Thi et al. 2001*a*) (see Figure 25). The sources were chosen to be isolated objects removed from molecular clouds, so that contamination from surrounding cloud emission is minimal. The S(1) and S(0) lines have been detected in several sources. Analysis of the data suggests that the mass of warm gas at ∼100-200 K is large, ranging from a few % to a significant fraction of the mass of the disks derived from the dust continuum, assuming a gas/dust ratio of 100. The origin of this warm gas is still a puzzle, although some of it could be due to heating of the surface layers of disks by stellar radiation if they have a warped geometry (e.g., Calvet et al. 1991, Chiang & Goldreich 1997).

Surprisingly, evidence for H_2 lines is also found toward three older Vega-type objects, including the debris-disk β Pictoris (Thi et al. 2001*b*). The data indicate residual primordial gas masses of 0.1–6 $M_{\rm Jupiter}$, much larger than inferred from CO, which freezes out onto grains in the disk mid-plane and is destroyed by photodissociation in the surface layers (Kamp & Bertoldi 2000). For β Pictoris, the gas mass of 0.1 $M_{\rm Jupiter}$ is insufficient to form new gaseous giant planets, but does affect the grain dynamics.

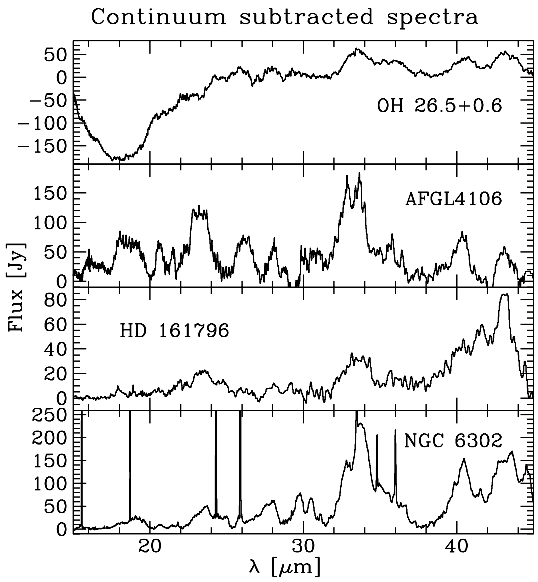

Figure 26. *The ISO-SWS 15-45 μm continuum-subtracted spectra of the AGB star OH 26.5+0.6 ($\lambda/\Delta\lambda \simeq$250), the red supergiant GL 4106 ($\lambda/\Delta\lambda \simeq$500), the protoplanetary nebulae HD 161796 ($\lambda/\Delta\lambda \simeq$250), and the planetary nebula NGC 6302 ($\lambda/\Delta\lambda \simeq$500), showing a host of features mainly attributed to olivine and pyroxene silicates. These spectra illustrate the incredible richness of the mid infrared spectra of circumstellar silicates and the detailed variations therein (Molster 2000).*

8. Circumstellar gas and dust around late-type stars

8.1. THE RICH SPECTRUM OF CIRCUMSTELLAR SILICATES

In the last phases of their lives, stars of moderate mass begin to pulsate and lose their outer layers, with the ejected material enriched in elements formed by nucleosynthesis inside stars. In the cooling outflow, solid particles such as silicates, oxides and carbonaceous material can condense, resulting in very rich mid-infrared spectra. The detection of the infrared emission from this circumstellar dust formed one cornerstone of the widespread acceptance of the importance of stardust for the interstellar dust budget (see §2.2). With the opening up of the telluric mid–infrared windows, the 10 and 18 μm features due to amorphous silicates around O–rich asymptotic giant branch (AGB) stars and the 12 μm feature due to SiC grains around C–rich AGB stars were quickly identified (Merrill & Stein 1976). That is where the field stalled until the launch of IRAS which had a low resolution spectrometer on board that took spectra at $R \approx 15 - 40$ from about 8 to 23 μm of many of such objects. While most showed these same dust features, some

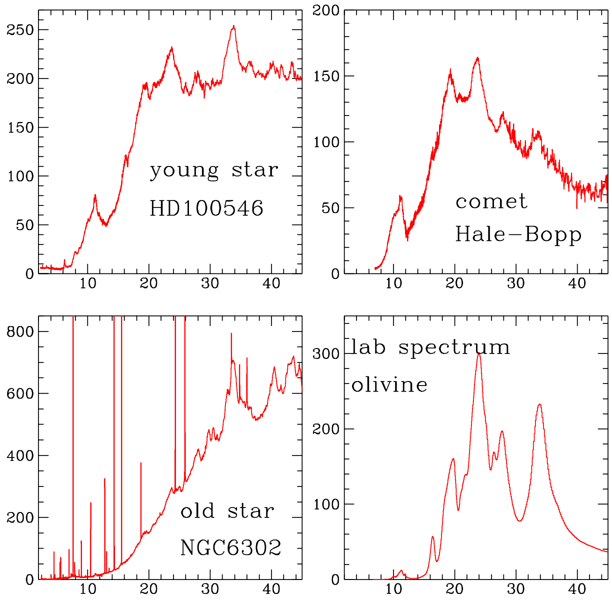

Figure 27. *The ISO-SWS mid–infrared spectra of newly formed stars, comets, and planetary nebulae show narrow emission features due to crystalline silicates (eg., forsterite and enstatite; Malfait et al. 1998, Molster 2000, Crovisier et al. 1997).*

spectra also revealed structure which was attributed to the presence of a small amount of crystalline silicates and to Al_2O_3 dust (e.g., Vardya et al. 1986).

One of the greatest surprises of the ISO mission was the incredible richness of the circumstellar silicate spectra at long wavelengths of AGB, post-AGB and planetary nebulae. Invariably, the 15-45 μm spectra of O–rich sources with circumstellar dust show a great number of narrow features, implying a crystalline carrier (Figure 26; Molster 2000). Based upon the laboratory studies of the infrared characteristics of crystalline silicates (Koike et al. 1993, 2000; Jäger et al. 1994, 1998), these features have been identified with crystalline olivine and pyroxene grains; specifically, fosterite (Mg_2SiO_4) and enstatite ($MgSiO_3$), the Mg–rich end members of the olivine and pyroxene families. The Fe/Mg abundance ratio is measured to be very low, less than 0.05. In contrast, circumstellar and interstellar amorphous silicates contain a substantial fraction of iron with Fe/Mg $\simeq$ 0.5 (Schutte & Tielens 1989, see §2.2).

These crystalline silicate features are ubiquitous and, besides O-rich AGB stars, post–AGB objects and planetary nebulae, they have now been observed in such diverse objects as luminous blue variables (i.e., AG Car), Herbig AeBe young stars, nominally C-rich objects such as the Red Rectangle and BD +30°3639, and comet Hale-Bopp (cf., Figure 27, Voors 1999, Crovisier et al. 1997, Malfait et al. 1998, Waters et al. 1998a,b, Molster 2000). Particularly, the Hale–Bopp spectrum is of interest since it shows almost exclusive presence of forsterite with very little enstatite and hence can serve as a template in the assignment of observed circumstellar silicate features.

Mass-losing O-rich AGB stars and related objects show evidence for a modest amount (1–10%) of crystalline silicates in their spectrum, whose origin is probably to be found in the condensation of the silicates near the star (Sylvester et al. 1999). A group of peculiar objects however, some of which are confirmed binaries, shows much higher crystalline silicate abundances (above 30%). These objects have stable, stationary disks and also show evidence for a population of large, cold grains. The large grains are likely the result of coagulation, a process which may eventually lead to cometesimals/planetesimals and eventually planets. Particularly, the contrast in crystallinity between the amorphous interstellar silicates, and the cold crystalline dust in the envelopes around late-type stars, YSOs and comets is puzzling; the more since the latter are generally thought to represent unprocessed interstellar material. It seems that silicates can anneal even at low temperatures – well below the glass temperature – on the long timescales and benign conditions provided by circumstellar disks (Molster et al. 1999).

8.2. DUST AROUND CARBON–RICH OBJECTS

The mid–infrared spectra of C–rich AGB, post–AGB and planetary nebulae show different dust emission features, reflecting a rich and diverse carbon-based chemistry. Much of this was hinted at already by the IRAS-LRS (Willems 1988, Kwok et al. 1989, Jourdain de Muizon et al. 1990) and followed up by the KAO (Buss et al. 1993, Omont et al. 1995) which revealed a feature at 21 μm (see below) and a feature near 30 μm in some objects. Figure 28 illustrates the ISO-SWS spectra for various C–rich stars. The AGB stars show a weak emission feature due to SiC at about 11.5 μm, which only for very extreme mass loss rates goes into absorption. Otherwise, besides a feature around 25 μm (see below), the infrared spectra are dominated by a featureless continuum, which is generally attributed to amorphous carbon (Martin & Rogers 1987). In the post–AGB phase, broad emission features at 8, 12, 20, and 25 μm radically change the spectral appearance. During this stage, weak PAH features at 6.2, 7.7, and 11.3 μm also appear. In the planetary nebulae phase, the PAH emission features dominate the 3-15 μm spectrum (cf., §3.2), while a 30 μm feature dominates at longer wavelengths

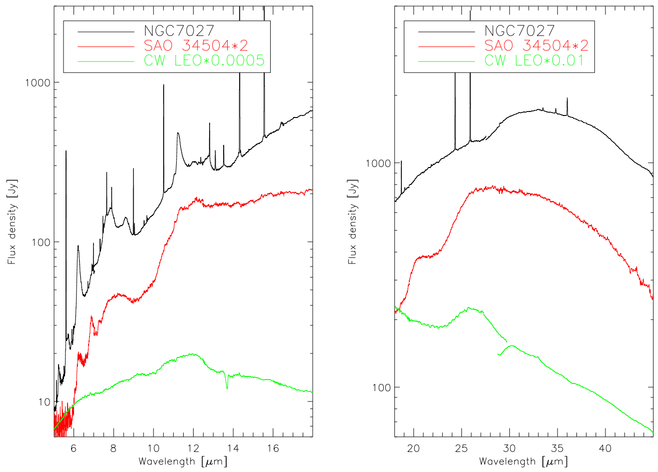

Figure 28. *A comparison of the 5–18 (left) and 18–45 μm ISO-SWS spectra of three C–rich objects: the AGB star IRC 10216/CW Leo (bottom), the post–AGB object IRAS 22272 (middle) — one of the so-called 21 μm objects (cf. §8.2)—, and the planetary nebula NGC 7027 (top). Note the strong spectral variation between these objects (Hony et al. 2000).*

(see below).

The feature near 21 μm has led to the identification of a class of sources known collectively as the "21μm sources" (Kwok et al. 1989). Visual spectroscopy has shown that these sources are metal–poor, C–rich, red giants with stellar temperatures in the range of 5000–8000 K and enhanced s–process element abundances, supporting their post-AGB nature (Hrivnak 1995, van Winckel & Reynier 2000). These population II stars with $M \approx 1$ $M_\odot$ were formed during the early history of the Milky Way and have now, after some 10^{10} yr, just reached the post–AGB phase which ends the life of all low mass stars. Hence, in an evolutionary sense, these objects are not directly related to the AGB and planetary nebulae objects shown in Figure 28. It has recently been shown that the 21 μm feature is well matched by the laboratory spectrum of TiC nanocrystals (Figure 29; von Helden et al. 2000). TiC was exclusively known as a circumstellar dust component through the discovery of small (200 Å) TiC cores inside graphitic stardust (Bernatowicz et al. 1996) and this is the first identification of this material in an astronomical object. Titanium is a very rare species and the presence of these dust grains requires very dense conditions for its formation in stellar ejecta. Hence, the 21 μm feature may signal dust formation during the extreme conditions associated with the superwind terminating the life of all low mass stars on the AGB and starting the transition to the planetary

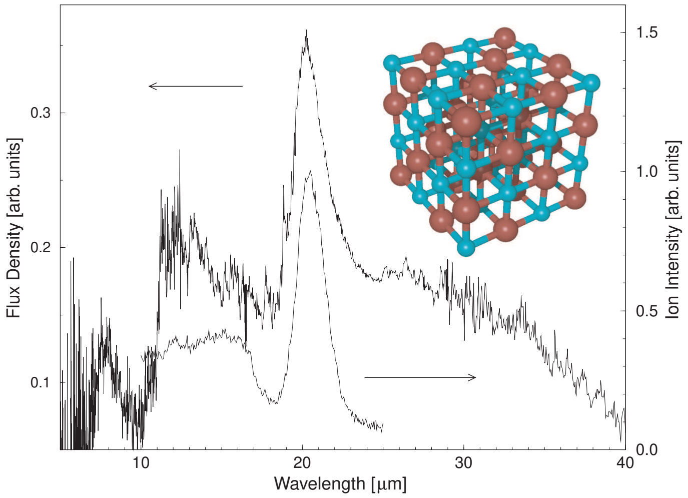

Figure 29. The emission spectrum from the post–AGB object SAO 96709, taken by the ISO satellite (upper trace, left axis) and the spectra of TiC nanocrystal clusters recorded in the laboratory (lower trace, right axis). Also shown is a pictorial representation of a typical (4x4x4 atom) TiC nanocrystal (von Helden et al. 2000).

nebula phase (Renzini 1987).

Traditionally, the strong band between 25 and 40 μm – shown by many C–rich AGB stars, post–AGB objects and planetary nebulae – has been called the 30 μm feature. This band has been tentatively assigned to solid MgS. Analysis of the SWS spectra shows that the band strongly changes both in shape and peak-position from the AGB to planetary nebulae phase (Figure 28). Comparison of its shape with laboratory measurements of solid MgS shows that this band cannot be explained by MgS grains alone. Likely, over time, the MgS is processed through its exposure to the harsh environment of the ejecta (Hony et al. 2000).

8.3. GAS TRACERS OF THE DUST CONDENSATION ZONE

A number of O-rich AGB stars, especially those that exhibit the dust emission band at 13 μm ascribed to Al_2O_3, show prominent, narrow emission lines between 13 and 16.5 μm in the ISO-SWS spectra. These have been identified as ro-vibrational transitions of CO_2 and $^{13}CO_2$ (Figure 30; Cami et al. 2000, Justtanont et al. 1996, 1998, Ryde et al. 1999), and this has been confirmed by high resolution Fabry-Perot observations. Synthetic spectra, assuming optically thin lines formed in LTE, compare well with the spectrum observed toward EP Aqr. The relatively high temperature ($\sim$ 650 K)

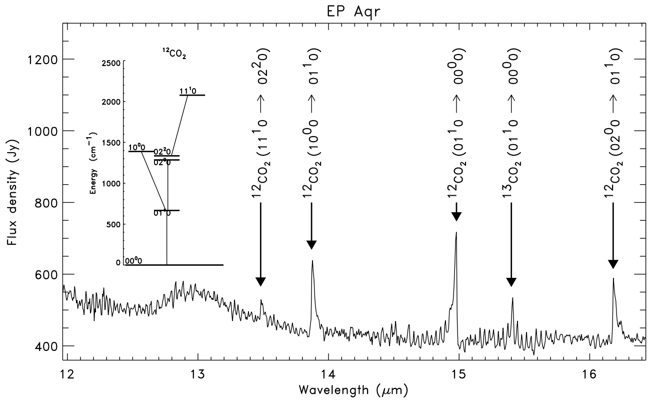

Figure 30. *The ISO-SWS 12–16 μm spectrum of the AGB star EP Aq, showing narrow emission features due to the Q-branches of the bending mode and various combination modes of gaeous CO_2 (see insert). Much of the structure in between is due to P- and R-branch transitions associated with these ro-vibrational modes (Cami et al. 2000).*

confirms the existence of a warm molecular envelope close to this type of stars; presumably the layer in which dust nucleates and the stellar wind originates.

ISO-SWS studies of the supergiants α Ori and α Sco revealed the presence of the fine-structure lines of [Si II] and [Fe II] (Justtanont et al. 1999). KAO studies had already shown the presence of intense [O I] 63 μm emission from these objects (Haas & Glassgold 1993). Analysis of the observed intensities shows that the emitting gas is dense ($> 10^6$ cm^{-3}), warm (1000 K), and located close to the star (< 20 R$_*$). Hence, these observations probe the region interior to the dust condensation zone for these supergiants. The observations are in good agreement with theoretical models for the heating and cooling and dynamics of these outflows (Rodgers & Glassgold 1991).

8.4. MOLECULAR EMISSION FROM AGB WINDS

AGB stars lose a large fraction of their mass through a cool, slowly expanding, stellar wind. The gas in this wind is heated through friction between the gas molecules and the radiatively accelerated dust grains which are driving the wind, and it cools through adiabatic expansion and molecular emission lines. This gas has been probed by rotational emission lines in the submillimeter from the ground and from the KAO. The ISO-LWS and SWS provided the first complete inventory of the dominant cooling lines of such winds. In O-rich objects, the cooling is dominated by H_2O (Figure 31; Barlow et al. 1996, Neufeld et al. 1996, Truong–Bach et al. 1999). The lines

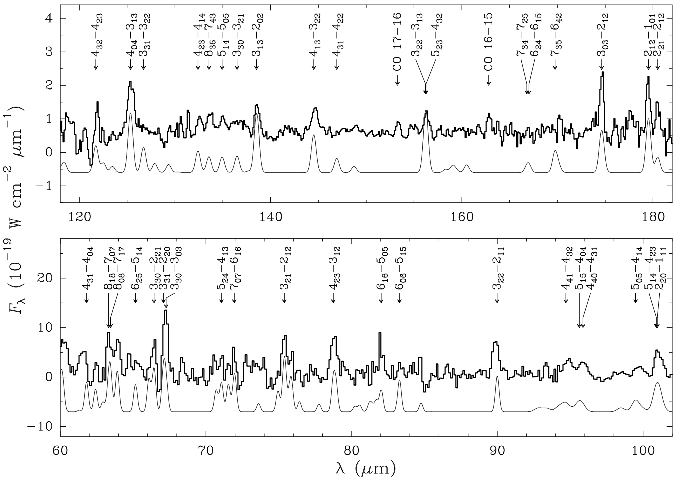

Figure 31. *Continuum-subtracted ISO-LWS spectrum of the O–rich AGB star W–Hya, showing a rich spectrum of rotational H_2O lines and a few CO lines (top trace). The dominant transitions are labelled on top. The bottom trace in each panel shows a model calculation for the water emission (Barlow et al. 1996).*

are highly optically thick and sensitive to the mass loss rate and the H_2O abundance, although for the shortest wavelength lines radiative pumping may affect the intensity as well (Barlow 1999). The emission spectrum of C–rich AGB stars, such as IRC +10216, is dominated by lines of CO and HCN (Cernicharo et al. 1996). Particularly, the HCN spectrum is very rich showing not only pure rotational transitions but also ro-vibrational transitions of low lying vibrational states. Because of this spectral richness, HCN dominates the cooling of these winds. At shorter wavelengths, many absorption bands due to carbon-chain molecules have been detected in absorption emphasizing a rich chemistry (Cernicharo 2000).

ISO-LWS spectra of C–rich post–AGB objects and planetary nebulae show high–lying pure rotational emission lines of CO (Cox et al. 1996, Liu et al. 1996, Justtanont et al. 1999). These lines were independently studied on the KAO (Justtanont et al. 1997). Detailed modeling shows that for the planetary nebula NGC 7027, the CO emission originates in a dense photodissociation region created by the stellar far-ultraviolet photons interacting with the previously ejected AGB wind. This warm and dense PDR is also probed by several pure-rotational lines of the CH^+ ion (Cernicharo et al. 1997), some of which were previously ascribed to H_2O. The CO emission in the spectrum of the post–AGB object, CRL 2688, in contrast, results from gas heated by the shock driven by the fast wind into the AGB ejecta. Future spectrally-resolved line profiles to be obtained with SOFIA and FIRST are needed to distinguish between the mechanisms.

9. Conclusions and future prospects

The airborne and space-based facilities of the past century have provided essential tools for studying the interstellar medium, star- and planet-forming regions and the envelopes around dying stars. Together, the spectral features allow a detailed picture of the lifecycle of the gas and dust from the quiescent ISM to YSOs to old stars to be developed, and, as a corollary, these features can now be used as diagnostic probes of the evolutionary states of objects. Laboratory spectroscopy has played an essential role in the development of the field, and continued support will be needed for future progress.

ISO has been highly successful in providing the first complete overview of the incredibly rich spectroscopy at infrared wavelengths, but has revealed —literally— only the "tip of the iceberg". The interpretation of the ISO data is severely hindered by insufficient spatial and spectral resolution, as well as sensitivity. What are the prospects to make the next leap forward in the coming decades? Due to the enormous progress in mid-infrared detector arrays and instrumentation, orders of magnitude improvement are still possible, provided that suitable air- and space-borne platforms are available. The SOFIA airplane will be well placed to pursue follow-up medium- and high-spectral resolution observations with a wide variety of instruments. The InfraRed Spectrometer (IRS) on SIRTF, operating at 5–40 μm, will have up to a factor of 100 better sensitivity than the ISO-SWS with moderate spectral resolution ($\lambda/\Delta\lambda$ =60–600) and will be very powerful to probe the solid-state features in objects which were too faint for ISO. FIRST will open up the terahertz frequency range ($\sim$ 60–500 μm) and the HIgh Frequency Instrument (HIFI) will provide spectrally resolved information on H_2O, high-J CO, and other atomic and molecular lines in the ISM and YSOs, whereas the Photoconducting Array Camera and Spectrometer (PACS) instrument will allow efficient mapping of atomic and molecular features at lower spectral resolution. Both SOFIA and FIRST will have considerably better spatial resolution than ISO and SIRTF. The largest gain in sensitivity and spatial resolution at mid-infrared wavelengths will potentially be provided by a camera and spectrometer on board NGST. ISO has paved the way for the exciting science to be performed with these and other new instruments in the coming century.

Acknowledgements

We would like to salute the dedicated work of all those responsible for building the superb infrared instruments on the various airborne and space-based platforms and getting them operational, including the Kuiper Airborne Observatory and the Infrared Space Observatory. We are also grateful to many colleagues and friends for providing preprints and comments, and for giving permission to reproduce their figures.

References

Abergel, A., Bernard, J.P., Boulanger, F., Cesarsky, C., Desert, F. X., Falgarone, E., Lagache, G., Perault, M., Puget, J.-L., Reach, W. T., Nordh, L., Olofsson, G., Huldtgren, M., Kaas, A. A., Andre, P., Bontemps, S., Burgdorf, M., Copet, E., Davies, J., Montmerle, T., Persi, P., Sibille, F. 1996, ISOCAM mapping of the ρ Ophiuchi main cloud, A&A, 315, L329–L333

Allamandola, L.J., Norman, C.A. 1978, Infrared emission lines from molecules in grain mantles, A&A, 63, L23–L26

Allamandola, L.J., Tielens, A.G.G.M., Barker, J.R. 1985, Polycyclic aromatic hydrocarbons and the unidentified infrared emission bands - Auto exhaust along the Milky Way, ApJ, 290, L25–L28

Allamandola, L.J., Sandford, S.A., Tielens, A.G.G.M., Herbst, T. 1992, Infrared spectroscopy of dense clouds in the C-H stretch region - Methanol and 'diamonds', ApJ, 399, 134–146

Allamandola, L.J., Tielens, A.G.G.M., Barker, J.R. 1989, Interstellar polycyclic aromatic hydrocarbons - The infrared emission bands, the excitation/emission mechanism, and the astrophysical implications, ApJS, 71, 733–775

Anders, E., Zinner, E. 1993, Interstellar grains in primitive meteorites - Diamond, silicon carbide, and graphite, Meteoritics, 28, 490–514

Andriesse, C.D. 1978, Platt particles in M 17, A&A, 66, 169–173

Bakes, E.L.O., Tielens, A.G.G.M. 1994, The photoelectric heating mechanism for very small graphitic grains and polycyclic aromatic hydrocarbons, ApJ, 427, 822–838

Baluteau, J.-P., Cox, P., Cernicharo, J., Pequignot, D., Caux, E., Lim, T., Swinyard, B., White, G., Kessler, M., Prusti, T., Barlow, M., Clegg, P. E., Emery, R. J., Furniss, I., Glencross, W., Gry, C., Joubert, M., Liseau, R., Nisini, B., Saraceno, P., Serra, G., Armand, C., Burgdorf, M., Digiorgio, A., Molinari, S., Price, M., Texier, D., Sidher, S., Trams, N. 1997, Detection of [O I] 63 μm in absorption toward SgrB2, A&A, 322, L33–L36

Barlow, M.J. 1999, ISO results on circumstellar envelopes, in Asymptotic Giant Branch Stars, eds. T. Le Bertre, A. Lebre, C. Waelkens, (ASP, San Francisco), 353

Barlow, M., Nguyen-Q-Rieu, Truong-Bach, Cernicharo, J., Gonzalez-Alfonso, E., Liu, X.-W., Cox, P., Sylvester, R. J., Clegg, P. E., Griffin, M. J., Swinyard, B. M., Unger, S. J., Baluteau, J.-P., Caux, E., Cohen, M., Cohen, R. J., Emery, R. J., Fischer, J., Furniss, I., Glencross, W. M., Greenhouse, M. A., Gry, C., Joubert, M., Lim, T., Lorenzetti, D., Nisini, B., Omont, A., Orfei, R., Pequignot, D., Saraceno, P., Serra, G., Skinner, C. J., Smith, H. A., Walker, H. J., Armand, C., Burgdorf, M., Ewart, D., di Giorgio, A., Molinari, S., Price, M., Sidher, S., Texier, D., Trams, N. 1996, The rich far-infrared water vapour spectrum of W Hya, A&A, 315, L241–L244

Barnard, E.E. 1919, On the dark markings of the sky, with a catalogue of 182 such objects, ApJ, 49, 1–24

Bauschlicher, C.W. 1998, The reaction of Polycyclic Aromatic Hydrocarbon cations with hydrogen atoms: the astrophysical implications, ApJ, 509, L125–L127

Beck, S.C., Lacy, J.H., Geballe, T.R. 1979, Detection of the 12.28 micron rotational line of molecular hydrogen in the Orion molecular cloud, ApJ, 234, L213–L216

Beckwith, S.V.W. Sargent, A.I. 1996, Circumstellar disks and the search for neighbouring planetary systems, Nature, 383, 139–144

Beckwith, S.V.M., Persson, S.E., Neugebauer, G., Becklin, E.E. 1978, Observations of the molecular hydrogen emission from the Orion nebula, ApJ, 223, 464–470

Bergin, E.A. Melnick, G.J., Stauffer, J.R., Ashby, M.L.N., Chin, G., Erickson, N.R., Goldsmith, P.F., Harwit, M., Howe, J.E., Kleiner, S.C., Koch, D.G., Neufeld, D.A., Patten, B.M., Plume, R., Schieder, R., Snell, R.L., Tolls, V., Wang, Z., Winnewisser, G., Zhang, Y. F. 2000, Implications of Submillimeter Wave Astronomy Satellite observations for interstellar chemistry and star formation, ApJ, 539, L133–L136

Bennett, C.J., Fixsen, D.J., Hinshaw, J.C., Mather, J. C., Moseley, S. H., Wright, E. L., Eplee, R. E., Jr., Gales, J., Hewagama, T., Isaacman, R. B., Shafer, R. A., Turpie, K. 1994, Morphology of the interstellar cooling lines detected by COBE, ApJ, 434, 587–598

Bernard, J.P., Boulanger, F., Désert, F.X., Giard, M., Helou, G., Puget, J. L. 1994, Dust emission of galactic cirrus from DIRBE observations, A&A, 291, L5–L8

Bernatowicz, T.J., Cowsik, R., Gibbons, P.C., Lodders, K., Fegley, B., Amari, S., Lewis, R.S. 1996, Constraints on stellar grain formation from presolar graphite in the Murchison meteorite, ApJ, 472, 760–782

Bertoldi, F., Timmermann, R., Rosenthal, D., Drapatz, S., Wright, C.M. 1999, Detection of HD in the Orion molecular outflow, A&A, 346, 267–277

Betz, A.L., Boreiko, R.T. 1989, Reversed far-infrared line emission from OH in Orion, ApJ, 346, L101–L104

Black, J.H. 1993, in The First Symposium on the Infrared Cirrus and Diffuse Interstellar Clouds, eds. R.M. Cutri, W.B. Latter, ASP Conf. Series Vol. 58 (ASP, San Francisco), p. 355

Black, J.H., van Dishoeck, E.F. 1987, Fluorescent excitation of interstellar H_2, ApJ, 322, 412–449

Blake, G.A., Keene, J., Phillips, T.G. 1985, Chlorine in dense interstellar clouds – The abundance of HCl in OMC-1, ApJ, 295, 501–506

Bless, R.C., Savage, B.D. 1972, Ultraviolet photometry from the Orbiting Astronomical Observatory. II. Interstellar extinction, ApJ, 171, 293–308

Bock, J.J., Hristov, V.V., Kawada, M. Matsuhara, H., Matsumoto, T., Matsuura, S., Mauskopf, P. D., Richards, P. L., Tanaka, M., Lange, A. E. 1993, Observation of forbidden C II 158 micron emission from the diffuse interstellar medium at high Galactic latitude, ApJ, 410, L115–L118

Bockelée-Morvan, D., Lis, D.C., Wink, J.E. Despois, D., Crovisier, J., Bachiller, R., Benford, D. J., Biver, N., Colom, P., Davies, J. K., Gérard, E., Germain, B., Houde, M., Mehringer, D., Moreno, R., Paubert, G., Phillips, T. G., Rauer, H. 2000, New molecules found in comet C/1995 O1 (Hale-Bopp). Investigating the link between cometary and interstellar material, A&A, 353, 1101–1114

Boland, W., de Jong, T. 1982, Carbon depletion in turbulent molecular cloud cores, ApJ, 261, 110–114

Boreiko, R.T., Betz, A.L. 1996a, The $^{12}C/^{13}C$ isotopic ratio in photodissociated gas in M42, ApJ, 467, L113–L116

Boreiko, R.T., Betz, A.L. 1996b, Heterodyne spectroscopy of the 63 micron [O I] Line in M42, ApJ, 464, L83–L86

Boogert, A.C.A., Schutte, W.A., Tielens, A.G.G.M., Whittet, D. C. B., Helmich, F. P., Ehrenfreund, P., Wesselius, P. R., de Graauw, T., Prusti, T. 1996, Solid methane toward deeply embedded protostars, A&A, 315, L377–L380

Boogert, A.C.A., Schutte, W.A., Helmich, F.P., Tielens, A.G.G.M., Wooden, D.H. 1997, Infrared observations and laboratory simulations of interstellar CH_4 and SO_2, A&A, 317, 929–941

Boogert, A.C.A., Helmich, F.P., van Dishoeck, E.F., Schutte, W.A., Tielens, A.G.G.M.,

Whittet, D.C.B. 1998, The gas/solid methane abundance ratio toward deeply embedded protostars A&A, 336, 352–358
Boogert, A.C.A., Ehrenfreund, P., Gerakines, P., Tielens, A. G. G. M., Whittet, D. C. B., Schutte, W. A., van Dishoeck, E. F., de Graauw, Th., Decin, L., Prusti, T. 2000, ISO-SWS observations of interstellar solid $^{13}CO_2$: heated ice and the Galactic $^{12}C/^{13}C$ abundance ratio, A&A, 353, 349–362
Boonman, A.M.S., van Dishoeck, E.F., Lahuis, F., Wright, C.M., Doty, S.D. 2000, Gas-phase H_2O and CO_2 towards massive protostars, in Analytical Spectroscopy with the ISO satellite, ESA-SP 456,
Boulanger, F. 1999, Dust emission and ISM components, in New Perspectives on the Interstellar Medium, eds. A.R. Taylor et al., ASP Series Vol. 168 (ASP, San Francisco), p. 173
Boulanger, F., Pérault, M. 1988, Diffuse infrared emission from the galaxy. I - Solar neighborhood, ApJ, 330, 964–985
Boulanger, F., Abergel, A., Bernard, J.-P., Burton, W. B., Desert, F.-X., Hartmann, D., Lagache, G., Puget, J.-L. 1996, The dust/gas correlation at high Galactic latitude, A&A, 312, 256–262
Burges, J.M., Thomas, R.N., eds., 1958, Proceedings of the 3rd symposium on Cosmical Gas Dynamics, Rev. Mod. Phys., 30, 1106-1107
Buss, R.H., Tielens, A.G.G.M., Cohen, M., Werner, M.W., Bregman, J.D., Witteborn, F.C. 1993, Infrared spectra of transition objects and the composition and evolution of carbon dust, ApJ, 415, 250–257
Cabrit, S., Bontemps, S., Lagage, P.O., Sauvage, M., Boulanger, F., André, P., Nordh, L., Olofsson, G., Cesarsky, C. J., de Boula, O., Sibille, F., Siebenmorgen, R. 1999, ISOCAM mapping and spectro-imaging of bipolar outflows, in The Universe as seen by ISO, eds. P. Cox, M.F. Kessler, ESA-SP 427, 449–452
Calvet, N., Patino, A., Magris, C., D'Alessio, P. 1991, Irradiation of accretion disks around young objects. I - Near-infrared CO bands, ApJ, 380, 617–630
Cami, J., et al. 2001, in preparation
Cardelli, J.A., Matthis, J.S., Ebbets, D.C., Savage, B.D. 1993, Abundance of interstellar carbon toward Zeta Ophiuchi, ApJ, 402, L17–L20
Carruthers, G.R. 1970, Rocket observation of interstellar molecular hydrogen, ApJ, 161, L81–L85
Caselli, P. Hasegawa, T.I., Herbst, E. 1993, Chemical differentiation between star-forming regions - the Orion Hot Core and Compact Ridge, ApJ, 408, 548–558
Ceccarelli, C., Castets. A., Loinard, L., Caux, E., Tielens, A.G.G.M. 1998a, Detection of doubly deuterated formaldehyde towards the low-luminosity protostar IRAS 16293-2422, A&A, 338, L43–L46
Ceccarelli, C., Caux, E., White, G.J., Molinari, S., Furniss, I., Liseau, R., Nisini, B., Saraceno, P., Spinoglio, L., Wolfire, M. 1998b, The far infrared line spectrum of the protostar IRAS 16293-2422, A&A, 331, 372–382
Ceccarelli, C., Hollenbach, D.J., Tielens, A.G.G.M. 1996, Far-infrared line emission from collapsing protostellar envelopes, ApJ, 471, 400–426
Cernicharo, J. 2000, ISO's view of the molecular content of evolved stars, in Astrochemistry: From Molecular Clouds to Planetary Systems, IAU Symposium 197, eds. Y.C. Minh & E.F. van Dishoeck (ASP, San Francisco), p. 375–390
Cernicharo, J., González-Alfonso, E., Alcolea, J., Bachiller, R., John, D. 1994, Widespread water vapor emission in Orion, ApJ, 432, L59–L62
Cernicharo, J., Lim, T., Cox, P., González-Alfonso, E., Caux, E., Swinyard, B. M., Martín-Pintado, J., Baluteau, J. P., Clegg, P. 1997, Widespread water vapour absorption in Sgr B2, A&A, 323, L25–L28
Cernicharo, J., Barlow, M.J., González-Alfonso, E. Cox, P., Clegg, P. E., Nguyen-Q-Rieu, Omont, A., Guelin, M., Liu, X.-W., Sylvester, R. J., Lim, T., Griffin, M. J., Swinyard, B. M., Unger, S. J., Ade, P. A. R., Baluteau, J.-P., Caux, E., Cohen, M., Emery, R. J., Fischer, J., Furniss, I., Glencross, W. M., Greenhouse, M. A., Gry, C., Joubert, M.,

Lorenzetti, D., Nisini, B., Orfei, R., Pequignot, D., Saraceno, P., Serra, G., Skinner, C. J., Smith, H. A., Towlson, W. A., Walker, H. J., Armand, C., Burgdorf, M., Ewart, D., di Giorgio, A., Molinari, S., Price, M., Sidher, S., Texier, D., Trams, N. 1996, The ISO/LWS far infrared spectrum of IRC+10 216, A&A, 315, L201–L204

Cernicharo, J., González-Alfonso, E., Sempere, M.J., Leeks, S. J., van Dishoeck, E. F., Wright, C. M., Lim, T., Cox, P., Perez-Martinez, S. 1999, The water vapour abundance and its spatial distribution in Orion and Sgr B2, in The Universe as seen by ISO, eds. P. Cox, M.F. Kessler, ESA-SP 427, 565–573

Cesarsky, D., Lequeux, J., Ryter, C., Gérin, M. 2000, ISO observations of the reflection nebula Ced 201: evolution of carbonaceous dust, A&A, 354, L87–L90

Cesarsky, D., Cox, P., Pineau des Forêts, G., van Dishoeck, E.F., Boulanger, F., Wright, C.M. 1999, ISOCAM spectro-imaging of the H_2 rotational lines in the supernova remnant IC 443, A&A, 348, 945–949

Charnley, S.B., Tielens, A.G.G.M., Millar, T.J. 1992, On the molecular complexity of the hot cores in Orion A - Grain surface chemistry as 'The last refuge of the scoundrel', ApJ, 399, L71–L74

Charnley, S.B. 1997, Sulfuretted molecules in hot cores, ApJ, 481, 396–405

Cheung, A.C., Rank, D.M., Townes, C.H., Thornton, D.D., Welch, W.J. 1968, Phys. Rev. Lett., 21, 1701

Chiang, E.I., Goldreich, P. 1997, Spectral energy distributions of T Tauri stars with passive circumstellar disks, ApJ, 490, 368–376

Chiang, E.I., Joung, M.K., Creech-Eakman, M.J., Qi, C., Kessler, J.E., Blake, G.A., van Dishoeck, E.F. 2000, Spectral energy distributions of T Tauri and Herbig Ae disks: grain mineralogy, parameter dependences, and comparison with ISO LWS Observations, ApJ, 547, 1077–1089

Chiar, J.E., Gerakines, P.A., Whittet, D.C.B., Pendleton, Y.L., Tielens, A.G.G.M., Adamson, A.J., Boogert, A.C.A. 1998, Processing of icy mantles in protostellar envelopes, ApJ, 498, 716–727

Chiar, J.E., Tielens, A.G.G.M., Whittet, D.C.B., Schutte, W. A., Boogert, A. C. A., Lutz, D., van Dishoeck, E. F., Bernstein, M. P. 2000, The composition and distribution of dust along the line of sight toward the Galactic Center, ApJ, 537, 749–762

Cox, P., Kessler, M., eds., 1999, The Universe as seen by ISO, ESA-SP 427 (ESTEC, Noordwijk)

Cox, P., González-Alfonso, E., Barlow, M.J., Liu, X.-W., Lim, T., Swinyard, B. M., Cernicharo, J., Omont, A., Caux, E., Gry, C., Griffin, M. J., Baluteau, J.-P., Clegg, P. E., Sidher, S., Pequignot, D., Nguyen-Q-Rieu, King, K. J., Ade, P. A. R., Towlson, W. A., Emery, R. J., Furniss, I., Joubert, M., Skinner, C. J., Cohen, M., Armand, C., Burgdorf, M., Eward, D., di Giorgio, A., Molinari, S., Texier, D., Trams, N., Unger, S. J., Glencross, W. M., Lorenzetti, D., Nisini, B., Orfei, R., Saraceno, P., Serra, G. 1996, The ISO/LWS spectrum of the Egg nebula, AFGL 2688, A&A, 315, L265–L268

Cox, P., Boulanger, F., Jones, A. 2000, in Les Houches summer school on ISO

Crovisier, J., Leech, K., Bockelée-Morvan, D., Brooke, T. Y., Hanner, M. S., Altieri, B., Keller, H. U., Lellouch, E. 1997, The spectrum of Comet Hale-Bopp (C/1995 01) observed with the Infrared Space Observatory at 2.9 AU from the Sun Science, 275, 1904–1907

Dartois, E., d'Hendecourt, L., Boulanger, F., Jourdain de Muizon, M., Breitfellner, M., Puget, J-L, Habing, H.J. 1998, Molecular gas phase counterparts to solid state grain mantles features: implication for gas/grain chemistry, A&A, 331, 651–660

de Graauw, Th., Whittet, D.C.B., Gerakines, P.A., Bauer, O. H., Beintema, D. A., Boogert, A. C. A., Boxhoorn, D. R., Chiar, J. E., Ehrenfreund, P., Feuchtgruber, H., Helmich, F. P., Heras, A. M., Huygen, R., Kester, D. J. M., Kunze, D., Lahuis, F., Leech, K. J., Lutz, D., Morris, P. W., Prusti, T., Roelfsema, P. R., Salama, A., Schaeidt, S. G., Schutte, W. A., Spoon, H. W. W., Tielens, A. G. G. M., Valentijn, E. A., Vandenbussche, B., van Dishoeck, E. F., Wesselius, P. R., Wieprecht, E., Wright, C. M. 1996, SWS observations of solid CO_2 in molecular clouds, A&A, 315,

L345–L348
Demyk, K., Dartois, E., d'Hendecourt, L., Jourdain de Muizon, M., Heras, A.M., Breitfellner, M. 1998, Laboratory identification of the 4.62 μm solid state absorption band in the ISO-SWS spectrum of RAFGL 7009S, A&A, 339, 553–560
Demyk, K., Jones, A. P., Dartois, E., Cox, P., D'Hendecourt, L. 1999, The chemical composition of the silicate dust around RAFGL7009S and IRAS 19110+1045, A&A, 349, 267–275
Désert, F.-X., Boulanger, F., Puget, J.L. 1990, Interstellar dust models for extinction and emission, A&A, 237, 215–236
d'Hendecourt, L.B., Jourdain de Muizon, M., 1989, The discovery of interstellar carbon dioxide, A&A, 223, L5–L8
d'Hendecourt, L.B., Léger, A. 1987, Effect of photoionization of PAH molecules on the heating of HI interstellar gas, A&A, 180, L9–L12
d'Hendecourt, L.B., Joblin, C., Jones, A. 1999a, eds., Solid Interstellar Matter: the ISO Revolution (EDP Sciences, Springer, Berlin)
d'Hendecourt, L.B., Jourdain de Muizon, M., Dartois, E. Breitfellner, M., Ehrenfreund, P., Benit, J., Boulanger, F., Puget, J. L., Habing, H. J. 1996, A&A, 315, L365–L368
d'Hendecourt, L., Jourdain de Muizon, M., Dartois, E., Demyk, K., Ehrenfreund, P., Heras, A.M. 1999b, SWS observations of protostars: the relevance of laboratory ices simulations, in The Universe as seen by ISO, eds. P. Cox & M.F. Kessler, ESA-SP 527, p. 589
Donn, B.D. 1968, Polycyclic Hydrocarbons, Platt particles, and interstellar extinction, ApJ, 152, L129–L132
Douglas, A.E., Herzberg, G. 1941, Note on CH^+ in interstellar space and in the laboratory, ApJ, 94, 381
Draine, B.T., Anderson, N. 1985, Temperature fluctuations and infrared emission from interstellar grains, ApJ, 292, 494–499
Draine, B.T., Bertoldi, F. 1999, Heating the gas in photodissociation regions, in The Universe as seen by ISO, eds. P. Cox, M.F. Kessler, ESA-SP 427, p. 553–559
Draine, B.T., McKee, C.F. 1993, Theory of interstellar shocks, ARAA, 31, 373–432
Duley, W.W., Williams, D.A. 1981, The infrared spectrum of interstellar dust - Surface functional groups on carbon, MNRAS, 196, 269–274
Duley, W.W., Williams, D.A. 1983, A 3.4 micron absorption band in amorphous carbon Implications for interstellar dust, MNRAS, 205, 67P–70P
Dutrey, A., Guilloteau, S., Duvert, G., Prato, L., Simon, M., Schuster, K., Menard, F. 1996, Dust and gas distribution around T Tauri stars in Taurus-Auriga. I. Interferometric 2.7mm continuum and ^{13}CO J=1–0 observations, A&A, 309, 493–504
Eddington, A.S. 1926, Proc. Roy. Soc. A, 111, 424
Eddy, J.A. 1972, J. Hist. Astron., 3, 165
Ehrenfreund, P., Charnley, S.B. 2000, Organic molecules in the interstellar medium, comets, and meteorites : a voyage from dark clouds to the early earth, ARAA, 38, 427–483
Ehrenfreund, P., Breukers, R., d'Hendecourt, L.B., Greenberg, J.M., 1992, On the possibility of detecting solid O_2 in interstellar grain mantles, A&A, 260, 431–436
Ehrenfreund, P., Schutte, W.A. 2000, Infrared observations of interstellar ices, in Astrochemistry: From Molecular Clouds to Planetary Systems, IAU Symposium 197, eds. Y.C. Minh & E.F. van Dishoeck (ASP, San Francisco), p. 135–146
Ehrenfreund, P., Dartois E., Demyk K., d'Hendecourt L. 1998, Ice segregation toward massive protostars, A&A, 339, L17–L20
Ehrenfreund, P., Kerkhof, O., Schutte, W.A., Boogert, A. C. A., Gerakines, P. A., Dartois, E., D'Hendecourt, L., Tielens, A. G. G. M., van Dishoeck, E. F., Whittet, D. C. B. 1999, Laboratory studies of thermally processed H_2O-CH_3OH-CO_2 ice mixtures and their astrophysical implication, A&A, 350, 240–253
Elitzur, M., Hollenbach, D.J., McKee, C.F. 1992, Planar H_2O masers in star-forming regions, ApJ 394, 221–227

Evans, N.J., Lacy, J.H., Carr, J.S. 1991, Infrared molecular spectroscopy toward the Orion IRc2 and IRc7 sources - A new probe of physical conditions and abundances in molecular clouds, ApJ, 383, 674–692

Ewen, H.I., Purcell, E.M. 1951, Nature, 168, 356

Field, G.B., Goldsmith, D.W., Habing, H.J. 1969, Cosmic-ray heating of the interstellar gas, ApJ, 155, L149–L154

Flower, D.R., Pineau des Forêts, G. 1999, H_2 emission from shocks in molecular outflows: the significance of departures from a stationary state, MNRAS, 308, 271–280

Fuente, A., Martín-Pintado, J., Rodríguez-Fernandez, N.J., Rodrí-Franco, A., de Vicente, P., Kunze, D. 1999, Infrared Space Observatory observations toward the reflection nebula NGC 7023: A nonequilibrium ortho-to-para-H_2 ratio, ApJ, 518, L45–L48

Gaustad, J.E. 1971, in Dark Nebulae, Globules and Protostars, ed. B.T. Lynds, (Univ. Arizona Press, Tucson), 91

Geballe, T.R., Tielens, A.G.G.M., Allamandola, L.J., Moorhouse, A. Brand, P.W.J.L. 1989, Spatial variations of the 3 micron emission features within UV-excited nebulae - Photochemical evolution of interstellar polycyclic aromatic hydrocarbons, ApJ, 341, 278–287

Genzel, R. 1992, in The Galactic Interstellar Medium, eds. D. Pfenniger & P. Bartholdi, Saas Fee Advanced Course 21 (Springer, Berlin), p. 275

Genzel, R., Stutzki, J. 1989, The Orion Molecular Cloud and star-forming region, ARAA, 27, 41–85

Gerakines, P.A., Whittet, D.C.B., Ehrenfreund, P., Boogert, A. C. A., Tielens, A. G. G. M., Schutte, W. A., Chiar, J. E., van Dishoeck, E. F., Prusti, T., Helmich, F. P., de Graauw, Th. 1999, Observations of solid carbon dioxide in molecular clouds with the Infrared Space Observatory, ApJ, 522, 357, erratum, 526, 1062

Giannini, T., Lorenzetti, D., Tommasi, E., Nisini, B., Benedettini, M., Pezzuto, S., Strafella, F., Barlow, M., Clegg, P. E., Cohen, M., di Giorgio, A. M., Liseau, R., Molinari, S., Palla, F., Saraceno, P., Smith, H. A., Spinoglio, L., White, G. J. 1999, ISO-LWS observations of Herbig Ae/Be stars. II. Molecular lines, A&A, 346, 617–625

Giard, M., Lamarre, J.M., Pajot, F., Serra, G. 1994, The large scale distribution of PAHs in the Galaxy, A&A, 286, 203–210

Gibb, E., Whittet, D.C.B., Gerakines, P.A., Boogert, A. C. A., Chiar, J. E., Ehrenfreund, P., Gerakines, P. A., Keane, J. V., Tielens, A. G. G. M., van Dishoeck, E. F., Kerkhof, O. 2000, An inventory of interstellar ices toward the embedded protostar W33A, ApJ, 347–356

Gillett, F.C., Forrest, W.J. 1973, Spectra of the Becklin-Neugebauer point source and the Kleinmann-low nebula from 2.8 to 13.5 microns, ApJ, 179, 483–491

Gillett, F.C., Jones, T.W., Merrill, K.M., Stein, W.A. 1975, Anisotropy of constituents of interstellar grains, A&A, 45, 77–81

Gilra, D.P. 1972, The scientific results from the Orbiting Astronomical Observatory OAO-2, ed A.D. Code, NASA SP-310, 297

Goldsmith, P.F., Melnick, G.J., Bergin, E.A., Howe, J.E., Snell, R.L., Neufeld, D.A., Harwit, M., Ashby, M.L.N., Patten, B.M., Kleiner, S.C., Plume, R., Stauffer, J.R., Tolls, V., Wang, Z., Zhang, Y.F., Erickson, N.R., Koch, D.G., Schieder, R., Winnewisser, G., Chin, G. 2000, O_2 in interstellar molecular clouds, ApJ, 539, L123–L126

Greenberg, J.M. 1982, Dust in dense clouds - one stage in a cycle, in Submillimeter Wave Astronomy, eds. J.E. Beckman & J.P. Phillips, (Cambridge Univ Press, Cambridge), 261–306

Greenberg, J.M., Hong, S.S. 1974, The chemical composition and distribution of interstellar grains, in Galactic Radio Astronomy, eds. F.J. Kerr & S.C. Simonson (Reidel, Dordrecht), p. 155–177

Greenberg, J.M., Muñoz-Caro, G. 2000, Organics in space: from interstellar dust to comets, in Astrochemistry: From Molecular Clouds to Planetary Systems, IAU Symposium 197, eds. Y.C. Minh & E.F. van Dishoeck (ASP, San Francisco), p. 331–342

Gry, C.J., Lequeux, J., Boulanger, F. 1992, Fine structure lines of C^+ and N^+ in the

galaxy, A&A, 266, 457–462
Haas, M.R., Glassgold, A.E. 1993, Detection of [O I] and [Si II] far-infrared fine-structure emission from Alpha Orionis, ApJ, 410, L111–L114
Haas, M.R., Davidson, J.A., Erickson, E.F., eds., 1995 Airborne Astronomy Symposium on the Galactic Ecosystem: From Gas to Stars to Dust, ASP Series vol. 73 (ASP, San Francisco)
Haas, M.R., Hollenbach, D.J., Erickson, E.F. 1991, Observations of forbidden [Si II] (35 microns) and [S I] (25 microns) in Orion - Evidence of a wind shock near IRc2, ApJ, 374, 555–563
Habing, H.J. 1968, Bull. Astr. Inst. Neth., 19, 421
Habing, H.J. 1989, The interstellar medium, in 'Evolution of galaxies and astronomical observations', proceedings of the first EADN Astrophysics School, eds. I. Appenzeller, H.J. Habing & P. Léna, p. 181–242
Hall, J.S. 1949, Science, 109, 166
Hartmann, D., Burton, W.B. 1997, Atlas of Galactic Neutral Hydrogen (Cambridge University Press)
Hartmann, J. 1904, Investigations on the spectrum and orbit of delta Orionis, ApJ, 19, 268–286
Hartquist, T.W., Williams, D.A. 1998, eds., The Molecular Astrophysics of Stars and Galaxies (Oxford University Press)
Harwit, M. 1999, Neugebauer, Martz & Leighton's observations of extremely cool stars, ApJ, 525, 1063–1064
Harwit, M., McNutt, D.P., Shivanandan, K., Zajac, B.J. 1966, Results of the first infrared astronomical rocket flight, AJ, 71, 1026–1029
Harwit, M., Neufeld, D.A., Melnick, G.J., Kaufman, M.J. 1998, Thermal water vapor emission from shocked regions in Orion, ApJ, 497, L105–L108
Heger, M.L. 1919, The occurrence of stationary D lines of sodium in the spectroscopic binaries, beta Scorpii and delta Orionis, Lick Obs. Bull., 326, 59–63
Heger, M.L. 1922, Further study of the sodium lines in class B stars, the spectra of certain class B stars in the regions 5630Å–6680Å and 3280Å–3380Å, Lick Obs. Bull, 337, 141–148
Heiles, C. 1994, On the origin of the diffuse C^+ 158 micron line emission, ApJ, 436, 720–727
Helmich, F.P., van Dishoeck, E.F., Black, J.H., de Graauw, T., Beintema, D. A., Heras, A. M., Lahuis, F., Morris, P. W., Valentijn, E. A. 1996, Detection of hot, abundant water toward AFGL 2591, A&A, 315, L173–L176
Heras, A.M., Leech, K., Trams, N.R., Perry, M., eds. 1997, First ISO Workshop on Analytical Spectroscopy, ESA-SP 419 (ESTEC, Noordwijk)
Hildebrand, R.H., Dragovan, M., Novak, G. 1984, Detection of submillimeter polarization in the Orion nebula, ApJ, 284, L51–L54
Hildebrand, R.H., Dotson, J.L., Dowell, C.D., Platt, S. R., Schleuning, David, Davidson, J. A., Novak, G. 1995, Far-infrared polarimetry, in Airborne Astronomy Symposium, eds. M. Haas. J.A. Davidson, E.F. Erickson, ASP Conf. Vol. 73 (ASP, San Francisco), p. 97
Hiltner, W.A. 1949, Science, 109, 165
Hollenbach, D.J. 1997, The physics of molecular shocks in YSO outflows, in Herbig-Haro Objects and the Birth of Low-mass Stars, IAU Symposium 182, ed. B. Reipurth & C. Bertout (Kluwer, Dordrecht), p. 181–198
Hollenbach, D.J., Tielens, A.G.G.M. 1997, Dense photodissociation regions (PDRs), ARAA 35, 179–216
Hollenbach, D.J., Tielens, A.G.G.M. 1999, Photodissociation regions in the interstellar medium of galaxies, Rev. Mod. Phys., 71, 173–230
Hollenbach, D.J., Chernoff, D.F., McKee, C.F. 1989, Infrared diagnostics of interstellar shocks, in Infrared Spectroscopy in Astronomy, 22'nd ESLAB Symposium, ed. B.H. Kaldeich, ESA-SP 290 (ESTEC, Noordwijk), p. 245–258

Hony, S., et al., 2000, in preparation
Hoyle, F., Wrickramasinghe, N.C. 1962, On graphite particles as interstellar grains, MNRAS, 124, 417–433
Hrivnak, B.J. 1995, Optical spectroscopy of carbon-rich proto-planetary nebulae, ApJ, 438, 341–349
Hudgins, D.M., Allamandola, L.J. 1999, Interstellar PAH Emission in the 11-14 Micron Region: New Insights from Laboratory Data and a Tracer of Ionized PAHs, ApJ, 516, L41–L44
Hudgins, D.M., Allamandola, L.J., 2000, in preparation
Irvine, W.M., Schloerb, F. P., Crovisier, J., Fegley, B., Jr., Mumma, M. J. 2000, Comets: a link between interstellar and nebular chemistry, in Protostars & Planets IV, eds. V. Mannings, A.P. Boss and S.S. Russell, (Univ. Arizona, Tucson), 1159–
Jaffe, D.T., Harris, A.I., Genzel, R. 1987, Warm dense gas in luminous protostellar regions - A submillimeter and far-infrared CO line study, ApJ, 316, 231–242
Jäger, C., Mutschke, H. Begemann, B., Dorschner, J., Henning, T. 1994, Steps toward interstellar silicate mineralogy. 1: Laboratory results of a silicate glass of mean cosmic composition, A&A, 292, 641–655
Jäger, C., Molster, F., Dorschner, J., Henning, Th., Mutschke, H., Waters, L.B.F.M. 1998, Steps toward interstellar silicate mineralogy. IV. The crystalline revolution, A&A, 339, 904–916
Joblin, C., Tielens, A.G.G.M., Allamandola, L.J., Geballe, T.R. 1996, Spatial variation of the 3.29 and 3.40 micron emission bands within reflection nebulae and the photochemical evolution of methylated Polycyclic Aromatic Hydrocarbons, ApJ, 458, 610–620
Joblin, C., Bregman J., Tielens, A.G.G.M., 2000, in preparation
Jones, A.P., Tielens, A.G.G.M., Hollenbach, D.J. 1996, Grain shattering in shocks: the interstellar grain size distribution, ApJ, 469, 740–764
Jourdain de Muizon, M., Cox P., Lequeux, J. 1990, A survey of infrared features in H II regions, planetary nebulae and proto-planetary nebulae from the IRAS-LRS data base, A&AS, 83, 337–355
Justtanont, K., de Jong, T., Helmich, F.P., Waters, L. B. F. M., de Graauw, T., Loup, C., Izumiura, H., Yamamura, I., Beintema, D. A., Lahuis, F., Roelfsema, P. R., Valentijn, E. A. 1996, The ISO-SWS spectrum of NML Cyg, A&A, 315, L217–L220
Justtanont, K., Tielens, A.G.G.M., Skinner, C.J., Haas, M.R. 1997, Observations of high rotational CO lines in post–asymptotic giant branch stars and planetary nebulae, ApJ, 476, 319–326
Justtanont, K., Feuchtgruber, H., de Jong, T., Cami, J., Waters, L.B.F.M., Yamamura, I., Onaka, T. 1998, Discovery of CO_2 emission in AGB stars with the 13μm dust feature, A&A, 330, L17–L20
Justtanont, K., Tielens, A.G.G.M., de Jong, T., Cami, J., Waters, L.B.F.M., Yamamura, I. 1999, Atomic fine-structure lines in the ISO-SWS spectra of the supergiants alpha Orionis and alpha Scorpii, A&A, 345, 605–610
Kamp, I., Bertoldi, F. 2000, CO in the circumstellar disks of Vega and β Pictoris, A&A, 353, 276–286
Kamijo, F. 1963, A theoretical study on the long period variable star, III. Formation of solid or liquid particles in the circumstellar envelope, PASJ, 15, 440–448
Kaufman, M.J., Neufeld, D.A. 1996, Far-infrared water emission from magnetohydrodynamic shock waves, ApJ, 456, 611–630
Kaufman, M.J., Wolfire, M.G., Hollenbach, D.J., Luhman, M.L. 1999, Far-infrared and submillimeter emission from galactic and extragalactic photodissociation regions, ApJ, 527, 795–813
Keane, J., et al., 2000, A&A, in press
Keene, J., Blake, G.A., Phillips, T.G., Huggins, P.J., Beichman, C.A. 1985, The abundance of atomic carbon near the ionization fronts in M17 and S140, ApJ, 299, 967–980
Keene, J., Lis, D.C., Phillips, T.G., Schilke, P., Werner, M.W., Zmuidzinas, J. 1999,

Atomic oxygen abundance from the dense ISM, in The Universe as seen by ISO, eds. P. Cox, M. Kessler ESA-SP 427, 687–689

Keene, J., Schilke, P., Kooi, J., Lis, D.C., Mehringer, D.M., Phillips, T.G. 1998, Detection of the $^3P_2$-$^3P_1$ submillimeter transition of ^{13}C I in the interstellar medium: implication for chemical fractionation, ApJ, 494, L107–L110

Kleinmann, D.E., Low, F.J. 1967, Discovery of an infrared nebula in Orion, ApJ, 149, L1–L4

Koerner, D.W., Sargent, A.I. 1995, Imaging the small-scale circumstellar gas around T Tauri stars, AJ, 109, 2138–2145

Koike, C., Shibai, H., Tuchiyama, A., 1993, Extinction of Olivine and Pyroxene in the mid infrared and far infrared, MNRAS, 264, 654–658

Koike, C., Tsuchiyama, A., Shibai, H., Suto, H., Tanabé, T., Chihara, H., Sogawa, H., Mouri, H., Okada, K. 2000, Absorption spectra of Mg-rich Mg-Fe and Ca pyroxenes in the mid- and far-infrared region, A&A, 363, 1115–1122

Kwok, S., Volk, K.M., Hrivnak, B.J. 1989, A 21 micron emission feature in four proto-planetary nebulae, ApJ, 345, L51–L54

Lacy, J.H., Carr, J.S., Evans, N.J., Baas, F., Achtermann, J.M., Arens, J.F. 1991, Discovery of interstellar methane - Observations of gaseous and solid CH_4 absorption toward young stars in molecular clouds, ApJ, 376, 556–560

Lacy, J.H., Evans, N.J., Achtermann, J.M., Bruce, D.E., Arens, J.F., Carr, J.S. 1989, Discovery of interstellar acetylene, ApJ, 342, L43–L46

Lacy, J.H., Faraji, H., Sandford, S.A., Allamandola, L.J. 1998, Unraveling the 10 micron "silicate" feature of protostars: the detection of frozen interstellar ammonia, ApJ, 501, L105–L108

Lahuis, F., van Dishoeck, E.F., 2000, ISO-SWS spectroscopy of gas-phase C_2H_2 and HCN toward massive young stellar objects, A&A, 355, 699–712

Langer, W.D., van Dishoeck, E.F., Bergin, E. A., Blake, G. A., Tielens, A. G. G. M., Velusamy, T., Whittet, D. C. B. 2000, Chemical evolution of protostellar matter, in Protostars & Planets IV, eds. V. Mannings, A.P. Boss and S.S. Russell, (Univ. Arizona, Tucson), 29–

Langhoff, S.R., 1996, J. Phys. Chem., 100, 2819

Le Bourlot, J., Pineau des Forêts, G., Roueff, E. 1995, Complex dynamical behaviour in interstellar clouds, A&A, 297, 251–260

Léger, A., Puget, J.L. 1984, Identification of the 'unidentified' IR emission features of interstellar dust?, A&A, 137, L5–L8

Li, A., Greenberg, J.M. 1997, A unified model of interstellar dust, A&A, 323, 566–584

Linsky, J.L. 1996, GHRS Observations of the LISM, Space Sci. Rev., 78, 157–164

Liseau, R., Ceccarelli, C., Larsson, B., Nisini, B., White, G. J., Ade, P., Armand, C., Burgdorf, M., Caux, E., Cerulli, R., Church, S., Clegg, P. E., Digorgio, A., Furniss, I., Giannini, T., Glencross, W., Gry, C., King, K., Lim, T., Lorenzetti, D., Molinari, S., Naylor, D., Orfei, R., Saraceno, P., Sidher, S., Smith, H., Spinoglio, L., Swinyard, B., Texier, D., Tommasi, E., Trams, N., Unger, S. 1996, Thermal H_2O emission from the Herbig-Haro flow HH 54, A&A, 315, L181–L184

Liu, X.-W., Barlow, M.J., Nguyen-Q-Rieu, Truong-Bach, Cox, P., Pequignot, D., Clegg, P. E., Swinyard, B. M., Griffin, M. J., Baluteau, J. P., Lim, T., Skinner, C. J., Smith, H. A., Ade, P. A. R., Furniss, I., Towlson, W. A., Unger, S. J., King, K. J., Davis, G. R., Cohen, M., Emery, R. J., Fischer, J., Glencross, W. M., Caux, E., Greenhouse, M. A., Gry, C., Joubert, M., Lorenzetti, D., Nisini, B., Omont, A., Orfei, R., Saraceno, P., Serra, G., Walker, H. J., Armand, C., Burgdorf, M., di Giorgio, A., Molinari, S., Price, M., Texier, D., Sidher, S., Trams, N. 1996, The ISO LWS grating spectrum of NGC 7027, A&A, 315, L257–L260

Lorenzetti, D., Tommasi, E., Giannini, T., Nisini, B., Benedettini, M., Pezzuto, S., Strafella, F., Barlow, M., Clegg, P. E., Cohen, M., di Giorgio, A. M., Liseau, R., Molinari, S., Palla, F., Saraceno, P., Smith, H. A., Spinoglio, L., White, G. J. 1999, ISO-LWS observations of Herbig Ae/Be stars. I. Fine-structure lines, A&A, 346, 604–

616
Malfait, K., Waelkens, C., Waters, L.B.F.M., Vandenbussche, B., Huygen, E., de Graauw, M. S. 1998, The spectrum of the young star HD 100546 observed with the Infrared Space Observatory, A&A, 332, L25–L28
Malfait, K., Waelkens, C., Bouwman, J., de Koter, A., Waters, L.B.F.M. 1999, The ISO spectrum of the young star HD 142527, A&A, 345, 181–186
Martin, P.G. 1989, Open panel discussion on interstellar grains models, in Interstellar Dust, eds. L.J. Allamandola & A.G.G.M. Tielens (Reidel, Dordrecht), 375
Martin, P.G., Rogers, C. 1987, Carbon grains in the envelope of IRC +10216, ApJ, 322, 374–392
Mathis, J.S., Rumpl, W., Nordsieck, K.H. 1977, The size distribution of interstellar grains, ApJ, 217, 425–433
Mattila, K., Lemke, D., Haikala, L.K., Laureijs, R. J., Leger, A., Lehtinen, K., Leinert, C., Mezger, P. G. 1996, Spectrophotometry of UIR bands in the diffuse emission of the galactic disk, A&A, 315, L353–L356
McCaughrean, M.J., O'Dell, R.C. 1996, Direct imaging of circumstellar disks in the Orion nebula AJ, 111, 1977–1986
McKee, C.F., Ostriker, J.P. 1977, A theory of the interstellar medium - Three components regulated by supernova explosions in an inhomogeneous substrate, ApJ, 218, 148–169
McKellar, A. 1940a, Evidence for the molecular origin of some hitherto unidentified interstellar lines, Publ. Astron. Soc. Pac., 52, 187–192
McKellar, A. 1940b, Wavelengths of the CH band lines, Publ. Astron. Soc. Pac., 52, 312–318
Melnick, G.J. 2000, First results from the Submillimeter Wave Astronomy Satellite — H_2O and O_2 discoveries, in Astrochemistry: From Molecular Clouds to Planetary Systems, IAU Symposium 197, eds. Y.C. Minh & E.F. van Dishoeck (ASP), p. 161–174
Melnick, G., Gull, G.E., Harwit, M. 1979, Observations of the 63 micron forbidden OI emission line in the Orion and Omega nebulae, ApJ, 227, L29–L33
Melnick, G.J., Genzel, R., Lugten, J.B. 1987, Interpretation of rotationally excited far-infrared OH emission in Orion-KL, ApJ, 321, 530–542
Melnick, G.J., Menten, K.M., Phillips, T.G., Hunter, T. 1993, Discovery of interstellar water lines at 437, 439 and 471 GHz: strong case for water maser formation behind C-type shocks, ApJ, 416, L37–L40
Melnick, G.J., Stauffer, J.R., Ashby, M.L.N., Bergin, E.A., Chin, G., Erickson, N.R., Goldsmith, P.F., Harwit, M., Howe, J.E., Kleuner, S.C., Koch, D.G., Neufeld, D.A., Patten, B.M., Plume, R., Schieder, R., Snell, R.L., Tolls, V., Wang, Z., Winnewisser, G., Zhang, Y.F. 2000, The Submillimeter Wave Astronomy Satellite: science objectives and instrument description, ApJ, 539, L77-L85
Merrill, P.W. 1934, Unidentified interstellar lines, Publ. Astron. Soc. Pac., 46, 206–207
Merrill, K.M., Stein, W.A. 1976, 2-14 μm stellar spectrophotometry. II. Stars from the 2 μm infrared sky survey, PASP, 88, 294–307
Meyer, M.R., Natta, A., Beckwith, S.V.W. 2000, Silicate emission in T Tauri stars: evidence for disk atmospheres? ApJ, in press
Minh, Y.C., van Dishoeck, E.F., eds. 2000, Astrochemistry: From Molecular Clouds to Planetary Systems, IAU Symposium 197 (ASP)
Mitchell, G.F., Maillard, J.–P., Allen, M., Beer, R., Belcourt, K. 1990, Hot and cold gas toward young stellar objects, ApJ, 363, 554–573
Molinari, S., Ceccarelli, C., White, G.J., Saraceno, P., Nisini, B., Giannini, T., Caux, E. 1999, Detection of the 62 μm crystalline H_2O ice feature in emission toward HH 7 with the ISO-LWS, ApJ, 521, L71–L74
Molster, F.J., Yamamura, I., Waters, L.B.F.M., Tielens, A. G. G. M., de Graauw, Th., de Jong, T., de Koter, A., Malfait, K., van den Ancker, M. E., Van Winckel, H., Voors, R. H. M., Waelkens, C. 1999, Low-temperature crystallization of silicate dust in circumstellar disks, Nature, 401, 563–

Molster, F.J., 2000, Ph.D. Thesis, Universiteit van Amsterdam
Moutou, C. C., Léger, A., d'Hendecourt, L., 1996, Far-infrared emission of PAH molecules (14-40μm): a preparation for ISO spectroscopy, A & A, 310, 297–308
Moutou, C., Verstraete, L., Léger, A., Sellgren, K., Schmidt, W., 2000, New PAH mode at 16.4 μm A&A, 354, L17–L20
Nakagawa, T., Yui, Y.Y., Doi, Y., Okuda, H., Shibai, H., Mochizuki, K., Nishimura, T., Low, F. 1998, Far-Infrared [C II] line survey observations of the Galactic plane ApJS, 115, 259–269
Neufeld, D.A., Kaufman, M.J. 1993, Radiative cooling of warm molecular gas, ApJ, 418, 263–272
Neufeld, D.A., Chen, W., Melnick, G.J., de Graauw, T., Feuchtgruber, H., Haser, L., Lutz, D., Harwit, M. 1996, Detection of far-infrared rotational lines of water vapour toward W Hydrae, A&A, 316, L237–L240
Nisini, B., Benedettini, M., Giannini, T., Caux, E., di Giorgio, A. M., Liseau, R., Lorenzetti, D., Molinari, S., Saraceno, P., Smith, H. A., Spinoglio, L., White, G. J. 1999, Strong H_2O and high-J CO emission towards the Class 0 protostar L1448-mm, A&A, 350, 529–540
Olofsson, G., Pagani, L., Tauber, J., Febvre, P., Deschamps, A., Encrenaz, P., Floren, H.-G., George, S., Lecomte, B., Ljung, B., Nordh, L., Pardo, J. R., Peron, I., Sjoekvist, M., Stegner, K., Stenmark, L., Ullberg, C. 1998, Low interstellar abundance of O_2 confirmed by the PIROG 8 balloon experiment, A&A, 339, L81–L84
Okuda, H., Matsumoto, T., Roellig, T.L., eds., 1997, The Diffuse Infrared Radiation and the IRTS, ASP Conf. Ser. vol. 124 (ASP, San Francisco)
Omont, A. 1986, Physics and chemistry of interstellar polycyclic aromatic molecules, A&A, 164, 159–178
Omont, A., Moseley, S.H., Cox, P., Glaccum, W., Casey, S., Forveille, T., Chan, Kin-Wing, Szczerba, R., Loewenstein, R. F., Harvey, P. M., Kwok, S. 1995, The 30 μm emission band in carbon-rich pre–planetary nebulae, ApJ, 454, 819–825
Palumbo, M.E., Geballe, T.R., Tielens, A.G.G.M. 1997, Solid carbonyl sulfide (OCS) in dense molecular clouds, ApJ, 479, 839–844
Palumbo, M.E., Pendleton, Y. J., Strazzulla, G. 2000, Hydrogen isotopic substitution studies of the 2165 wavenumber (4.62 Micron) "XCN" feature produced by ion bombardment, ApJ, 542, 890–893
Parmar, P.S., Lacy, J.H., Achtermann, J.M. 1991, Detection of low-J pure-rotational emission from H_2 in the Orion Bar region - evidence for small-scale clumpiness, ApJ, 372, L25–L28
Peeters, E., Tielens, A.G.G.M., Roelfsema, P.R., Cox, P. 1999, PAHs in compact HII regions, in The Universe as seen by ISO, eds. P. Cox, M.F. Kessler, (ESA, Noordwijk), ESA SP–427, 739–741
Pendleton, Y.J., Cruikshank, D.P. 1994, Life from the stars?, Sky & Telescope, 87, 36
Pendleton, Y., Tielens, A.G.G.M., Tokunaga, A.T., Bernstein, M.P., 1999, The Interstellar 4.62 μm band, ApJ, 513, 294–304
Pendleton, Y.J., Sandford, S.A., Allamandola, L.J., Tielens, A.G.G.M., Sellgren, K. 1994, Near-infrared absorption spectroscopy of interstellar hydrocarbon grains, ApJ, 437, 683–696
Phillips, T.G., Huggins, P.J., Kuiper, T.B.H., Miller, R.E. 1980, Detection of the 610 μm (492 GHz) line of interstellar atomic carbon, ApJ, 238, L103–L106
Phillips, T.G., Kwan, J., Huggins, P.J. 1980, Detection of submillimeter lines of CO at 0.65 mm and H_2O at 0.79 mm, in Interstellar Molecules, IAU Symposium, ed. B.H. Andrews, p. 21–24
Phillips, T.G., Scoville, N.Z., Kwan, J., Huggins, P.J., Wannier, P.G. 1978, Detection of $H_2^{18}O$ and an abundance estimate for interstellar water, ApJ, 222, L59–L62
Platt, J.R. 1956, On the optical properties of interstellar dust, ApJ, 123, 486–490
Pottasch, S.R., Wesselius, P.R., van Duinen, R.J. 1979, Determination of cooling rates in the interstellar medium, A&A, 74, L15–L17

Purcell, E.M. 1976, Temperature fluctuations in very small interstellar grains, ApJ, 206, 685–690

Reach, W.T., Dwek, E., Fixsen, D.J., Hewagama, T., Mather, J. C., Shafer, R. A., Banday, A. J., Bennett, C. L., Cheng, E. S., Eplee, R. E., Jr., Leisawitz, D., Lubin, P. M., Read, S. M., Rosen, L. P., Shuman, F. G. D., Smoot, G. F., Sodroski, T. J., Wright, E. L. 1995, Far-infrared spectral observations of the Galaxy by COBE, ApJ, 451, 188–199

Renzini, A. 1987, in Physical Processes in Red Giants, eds. I. Iben & A. Renzini, (Reidel, Dordrecht), 431

Rodgers, B., Glassgold, A.E. 1991, The temperature of the circumstellar envelope of Alpha Orionis, ApJ, 382, 606–616

Roelfsema, P., Cox, P., Tielens, A.G.G.M., Allamandola, L. J., Baluteau, J.-P., Barlow, M. J., Beintema, D., Boxhoorn, D. R., Cassinelli, J. P., Caux, E., Churchwell, E., Clegg, P. E., de Graauw, T., Heras, A. M., Huygen, R., van der Hucht, K. A., Hudgins, D. M., Kessler, M. F., Lim, T., Sandford, S. A. 1996, SWS observations of IR emission features towards compact HII regions, A&A, 315, L289–L292

Rosenthal, D., Bertoldi, F., Drapatz, S. 2000, ISO-SWS observations of OMC-1: H_2 and fine structure lines, A&A, 356, 705–723

Rowan-Robinson, M. 1992, Interstellar dust in galaxies, MNRAS, 258, 787–799

Russell, R.W., Melnick, G., Gull, G.E., Harwit, M. 1980, Detection of the 157 micron (1910 GHz) [C II] emission line from the interstellar gas complexes NGC 2024 and M42, ApJ, 240, L99–L102

Russell, R.W., Soifer, B.T., Willner, S.P., 1977, The 4 to 8 micron spectrum of NGC 7027, ApJ, 217, L149–L152

Ryde, N., Eriksson, K., Gustafsson, B. 1999, The nature of the circumstellar CO_2 emission from M giants, A&A, 341, 579–586

Salama, A. et al. eds. 2000, ISO beyond the Peaks, Second ISO Workshop on Analytical Spectroscopy, ESA-SP 456 (ESTEC, Noordwijk)

Saraceno, P., Benedettini, M., Di Giorgio, A.M., Giannini, T., Nisini, B., Lorenzetti, D., Molinari, S., Pezzuto, S., Spinoglio, L., Tommasi, E., Clegg, P. E., Correia, J. C., Griffin, M. J., Kaufman, M. J., Leeks, S. J., White, G. J., Caux, E., Liseau, R., Smith, H. 1999, ISO-LWS study of pre-main sequence sources, in Physics and Chemistry of the Interstellar Medium III, eds. V. Ossenkopf et al. (GCA Verlag, Herdecke), p. 279

Schutte, W.A., Boogert, A.C.A., Tielens, A.G.G.M., Whittet, D. C. B., Gerakines, P. A., Chiar, J. E., Ehrenfreund, P., Greenberg, J. M., van Dishoeck, E. F., de Graauw, Th. 1999, Weak ice absorption features at 7.24 and 7.41 μm in the spectrum of the obscured young stellar object W 33A, A&A, 343, 966–976

Schutte, W.A., Greenberg, J.M., 1997, Further evidence for the OCN^- assignment to the XCN band in astrophysical ice analogs, A&A, 317, L43–L46

Schutte, W.A., Tielens, A.G.G.M. 1989, Theoretical studies of the infrared emission from circumstellar dust shells - The infrared characteristics of circumstellar silicates and the mass-loss rate of oxygen-rich late-type giants, ApJ, 343, 369–392

Schutte, W.A., Tielens, A.G.G.M., Whittet, D.C.B., Boogert, A., Ehrenfreund, P., de Graauw, T., Prusti, T., van Dishoeck, E. F., Wesselius, P. 1996, The 6.0 and 6.8μm absorption features in the spectrum of NGC 7538:IRS9, A&A, 315, L333–L336

Sellgren, K. 1984, The near-infrared continuum emission of visual reflection nebulae, ApJ, 277, 623–633

Shibai, H., Okuda, H., Nakagawa, T., Matsuhara, H., Maihara, T., Mizutani, K., Kobayashi, Y., Hiromoto, N., Nishimura, T., Low, F.J. 1991, Large-scale forbidden [C II] 158 μm emission from the Galaxy, ApJ, 374, 522–532

Sitko, M.L., Grady, C.A., Lynch, D.K., Russell, R.W., Hanner, M.S. 1999, Cometary Dust in the debris disks of HD 31648 and HD 163296: two “baby” beta Pictoris stars, ApJ, 510, 408–412

Snell, R.L., Howe, J. E., Ashby, M. L. N., Bergin, E. A., Chin, G., Erickson, N. R., Goldsmith, P. F., Harwit, M., Kleiner, S. C., Koch, D. G., Neufeld, D. A., Patten,

B. M., Plume, R., Schieder, R., Stauffer, J. R., Tolls, V., Wang, Z., Winnewisser, G., Zhang, Y. F., Melnick, G. J. 2000, Water abundance in molecular cloud cores, ApJ, 539, L101–L104

Snow, T.P., 1995, A Critique of Suggested Diffuse Band Carriers, in The Diffuse Interstellar Bands, eds. A.G.G.M. Tielens & T.P. Snow, (Kluwer, Dordrecht), 379

Sodroski, T.J., Bennett, C., Boggess, N., Dwek, E., Franz, B. A., Hauser, M. G., Kelsall, T., Moseley, S. H., Odegard, N., Silverberg, R. F., Weiland, J. L. 1994, Large-scale characteristics of interstellar dust from COBE–DIRBE observations, ApJ, 428, 638–646

Spaans, M., van Dishoeck, E.F. 2001, The abundance and emission of H_2O and O_2 in clumpy molecular clouds, ApJ, 548, L217–L220

Spinoglio, L., Giannini, T., Nisini, B., van den Ancker, M. E., Caux, E., Di Giorgio, A. M., Lorenzetti, D., Palla, F., Pezzuto, S., Saraceno, P., Smith, H. A., White, G. J. 2000, Shock excited far-infrared molecular emission around T Tau, A&A, 353, 1055–1064

Spitzer, L. 1978, Physicial Processes in the Interstellar Medium (Wiley, New York)

Spitzer, L., Jenkins, E.B. 1975, Ultraviolet studies of the interstellar gas, ARAA, 13, 133–164

Stacey, G.J., Jaffe, D.T., Geis, N., Grenzel, R., Harris, A. I., Poglitsch, A., Stutzki, J., Townes, C. H. 1993, 158 μm forbidden [C II] mapping of the Orion molecular cloud, ApJ, 404, 219–231

Stacey, G.J., Kurtz, N.T., Smyers, S.D., Harwit, M., Russell, R.W., Melnick, G. 1982, The mass of hot, shocked CO in Orion — first observations of the J =17–J =16 transition at 153 μm, ApJ, 257, L37–L40

Stacey, G.J., Smyers, S.D., Kurtz, N.T., Harwit, M. 1983, Observations of the 145.5 μm [O I] forbidden emission line in the Orion nebula, ApJ, 265, L7–L11

Stacey, G.J., Viscuso, P.J., Fuller, C.E., Kurtz, N.T. 1985, The 157 μm forbidden [C II] luminosity of the Galaxy. II - The presence of knotlike features in the forbidden [C II] emission, ApJ, 289, 803–806

Stapelfeldt, K., Padgett, D., Brooke, T.Y. 1999, A survey for H_2 rotational emission in low-mass pre-main sequence stars, in The Universe as seen by ISO, eds. P. Cox & M.F. Kessler, ESA-SP 427, p. 525

Stecher, T.P. 1965, Interstellar extinction in the ultraviolet, ApJ, 142, 1683–1684

Stein, W.A., 1967, in Interstellar Grains, eds. J.M. Greenberg & T.P. Roark, NASA SP-140, 185

Sternberg, A., Dalgarno, A. 1989, The infrared response of molecular hydrogen gas to ultraviolet radiation — High-density regions, ApJ, 338, 197–233

Storey, J.W.V., Watson, D.M., Townes, C.H. 1979, Observations of far-infrared fine structure lines — Forbidden [O III] 88.35 μm and forbidden [O I] 63.2 μm, ApJ, 233, 109–118

Stutzki, J., Stacey, G.J., Genzel, R., Harris, A.I., Jaffe, D.T., Lugten, J.B. 1988, Submillimeter and far-infrared line observations of M17 SW - A clumpy molecular cloud penetrated by ultraviolet radiation, ApJ, 332, 379–399

Swings, P., Rosenfeld, L. 1937, Considerations regarding interstellar molecules, ApJ, 86, 483–486

Sylvester, R.J., Kemper, F., Barlow, M.J., de Jong, T., Waters, L.B.F.M., Tielens, A.G.G.M., Omont, A. 1999, A&A, 2.4-197 μm spectroscopy of OH/IR stars: the IR characteristics of circumstellar dust in O-rich environments, 352, 587–599

Szczepanski, J., Vala, M. 1993, Laboratory evidence for ionized polycyclic aromatic hydrocarbons in the interstellar medium, Nature, 363, 699–701

Telesco, C.M., Knacke, R.F. 1991, Detection of silicates in the beta Pictoris disk, ApJ, 372, L29–L31

Thi, W.F., van Dishoeck, E.F., Jansen, D.J., Spaans, M., Li, W., Evans, N.J., Jaffe, D.T. 1997, Weak H_2 emission from diffuse and translucent clouds, in First ISO Workshop on Analytical Spectroscopy, ESA SP-419, p. 299

Thi, W.F., van Dishoeck, E.F., Blake, G.A., van Zadelhoff, G.J., Hogerheijde, M.R. 1999a,

Detection of H_2 pure rotational line emission from the GG Tauri binary system, ApJ, 521, L63–L66
Thi, W.F., van Dishoeck, E.F., Blake, G.A., van Zadelhoff, G. J., Hogerheijde M. R., Mannings, V., Sargent, A. I., Becklin, E. E., Horn, J., Zuckerman, B., Koerner, D., Mundy, L. G., Waters, L. B. F. M., Wesselius, P. R., van den Ancker, M. E., Natta, A., Waelkens, C., Malfait, K. 1999b, H_2 emission from disks around Herbig Ae and T Tauri stars, in The Universe as seen by ISO, eds. P. Cox, M.F. Kessler, ESA-SP 427, p. 529–532
Thi, W.F., Blake, G.A., van Dishoeck, E.F., van Zadelhoff, G.J., Horn, J., Becklin, E.E., Mannings, V., Sargent, A.I., van den Ancker, M.E., Natta, A. 2001a, Substantial reservoirs of molecular gas in the debris disks around young stars, Nature, 409, 60–63
Thi, W.F., van Dishoeck, E.F., Blake, G.A., van Zadelhoff, G.J., Horn, J., Becklin, E.E., Mannings, V., Sargent, A.I., van den Ancker, M.E., Natta, A. 2001b, H_2 and CO emission from disks around T Tauri and Herbig Ae stars and debris-disk objects: cold and warm circumstellar gas, ApJ, in press
Tielens, A.G.G.M. 1983, Surface chemistry of deuterated molecules, A&A, 119, 177–184
Tielens, A.G.G.M. 1995, The Interstellar Medium, in Airborne Astronomy Symposium, eds. M.R. Haas, J.A. Davidson, E.F. Erickson (ASP, San Francisco), p 3–22
Tielens, A.G.G.M. 1997, Heating and cooling of the interstellar medium, in Diffuse Infrared Radiation and the IRTS, eds. H. Okuda, T. Matsumoto, T.L. Roellig (Kluwer, Dordrecht), p. 255
Tielens, A.G.G.M. 1999, The destruction of interstellar dust, in Formation and Evolution of Solids in Space, eds. J.M. Greenberg & A. Li (Kluwer, Dordrecht), p. 331
Tielens, A.G.G.M., Allamandola, L.J., 1987a, Composition, structure, and chemistry of interstellar dust, in Interstellar Processes, eds. D.J. Hollenbach & H.A. Thronson (Reidel, Dordrecht), p. 397–469
Tielens, A.G.G.M., Allamandola, L.J., 1987b, Evolution of interstellar dust, in Physical Processes in Interstellar Clouds, eds. G. Morfill & M. Scholer (Reidel, Dordrecht), p. 333–376
Tielens, A.G.G.M., Hagen, W. 1982, Model calculations of the molecular composition of interstellar grain mantles, A&A, 114, 245–260
Tielens, A.G.G.M., Hollenbach, D.J. 1985a, Photodissociation regions. I. Basic model. ApJ, 291, 722–746
Tielens, A.G.G.M., Hollenbach, D.J. 1985b, Photodissociation regions. II. A model for the Orion photodissociation region, ApJ, 291, 747–754
Tielens, A.G.G.M., Whittet, D.C.B. 1997, Interstellar ices, in Molecules in Astrophysics: Probes and Processes, IAU Symposium 178, ed. E.F. van Dishoeck (Kluwer, Dordrecht), p. 48
Tielens, A.G.G.M., Hony, S., van Kerckhoven, C., Peeters, E. 1999, Interstellar and circumstellar PAHs, in The Universe as seen by ISO, eds. P. Cox & M.F. Kessler, ESA SP-427, 579–587
Tielens, A.G.G.M., Hony, S., van Kerckhoven, C., Peeters, E. 2000, Interstellar and circumstellar PAHs, in Astrochemistry: From Molecular Clouds to Planetary Systems, IAU Symposium 197, eds. Y.C. Minh & E.F. van Dishoeck (ASP, San Francisco), p. 349–362
Tielens, A.G.G.M., Tokunaga, A.T., Geballe, T.R., Baas, F. 1991, Interstellar solid CO — Polar and nonpolar interstellar ices, ApJ, 381, 181–199
Tielens, A.G.G.M., Wooden, D.H., Allamandola, L.J., Bregman, J., Witteborn, F.C. 1996, The infrared spectrum of the Galactic center and the composition of interstellar dust, ApJ, 461, 210–222
Timmermann, R., Bertoldi, F., Wright, C.M., Drapatz, S., Draine, B.T., Haser, L., Sternberg, A. 1996, H_2 infrared line emission from S 140: a warm PDR, A&A, 315, L281–L284
Trumpler, R.J. 1930, Preliminary results on the distances, dimensions and space distribution of open star clusters, Lick Obs. Bull., 420, 154–188

Truong–Bach, R.J., Sylvester, R.J., Barlow, M.J. Nguyen-Q-Rieu, Lim, T., Liu, X. W., Baluteau, J. P., Deguchi, S., Justtanont, K., Tielens, A. G. G. M. 1999, H_2O from R Cas: ISO LWS-SWS observations and detailed modelling, A&A, 345, 925–935

Turner, B.E. 1990, Detection of doubly deuterated interstellar formaldehyde (D_2CO) - an indicator of active grain surface chemistry, ApJ, 362, L29–L33

van de Hulst, H.C. 1949, The solid particles in interstellar space, Rech. Astr. Obs. Utrecht, 11, part 2

van de Hulst, H,C. 1997, Molecules in astrophysics half a century ago, in Molecules in Astrophysics: Probes and Processes, ed. E.F. van Dishoeck (Kluwer, Dordrecht), p. 13

van den Ancker, M.E., Wesselius, P.R., Tielens, A.G.G.M. 2000a, ISO spectroscopy of young intermediate-mass stars in the BD+40°4124 group, A&A, 355, 194–210

van den Ancker, M.E., Tielens, A.G.G.M., Wesselius, P.R. 2000b, ISO Spectroscopy of the young bipolar nebulae S106 IR and Cep A East, A&A, 358, 1035–1048

van den Ancker, M.E., Bouwman, J., Wesselius, P.R., Waters, L.B.F.M., Dougherty, S.M., van Dishoeck, E.F. 2000c, ISO spectroscopy of circumstellar dust in the Herbig Ae systems AB Aur and HD 163296, A&A, 357, 325–329

Vandenbussche, B., Ehrenfreund, P., Boogert, A.C.A., van Dishoeck, E. F., Schutte, W. A., Gerakines, P. A., Chiar, J., Tielens, A. G. G. M., Keane, J., Whittet, D. C. B., Breitfellner, M., Burgdorf, M. 1999, Constraints on the abundance of solid O_2 in dense clouds from ISO-SWS and ground-based observations, A&A, 346, L57–L60

van der Tak, F.F.T., van Dishoeck, E.F., Evans, N.J., Blake, G.A. 2000, Structure and evolution of the envelopes of deeply embedded massive young stars, ApJ, 537, 283–303

van Dishoeck, E.F. 1998, What can ISO tell us about gas-grain chemistry? Faraday Discussion, 109, 31–

van Dishoeck, E.F., Black, J.H. 1988, The photodissociation and chemistry of interstellar CO, ApJ, 334, 771–802

van Dishoeck, E.F., Blake, G.A. 1998, Chemical evolution of star-forming regions, ARAA, 36, 317–368

van Dishoeck, E.F., Helmich, F.P. 1996, Infrared absorption of H_2O toward massive young stars, A&A, 315, L177–L180

van Dishoeck, E.F., Hogerheijde, M.R. 1999, Models and observations of the chemistry near young stellar objects, in Origins of Stars and Planetary Systems, eds. C.J. Lada & N. Kylafis (Kluwer, Dordrecht), p. 97–

van Dishoeck, E.F., van der Tak, F.F.S. 2000, Chemistry in the envelopes around massive young stars, Astrochemistry: From Molecular Clouds to Planetary Systems, IAU Symposium 197, eds. Y.C. Minh & E.F. van Dishoeck (ASp, San Francisco), p. 97–112

van Dishoeck, E.F., Black, J.H., Boogert, A.C.A., Boonman, A. M. S., Ehrenfreund, P., Gerakines, P. A., de Graauw, Th., Helmich, F. P., Keane, J. V., Lahuis, F., Schutte, W. A., Tielens, A. G. G. M., Whittet, D. C. B., Wright, C. M., van den Ancker, M. E., Blake, G. A., Creech-Eakman, M., Waters, L. B. F. M., Wesselius, P. R. 1999, ISO spectroscopy of young stellar objects, in The Universe as seen by ISO, eds. P. Cox & M.F. Kessler, ESA SP-427, p. 437–448

van Dishoeck, E.F., Helmich, F.P., de Graauw, Th. Black, J. H., Boogert, A. C. A., Ehrenfreund, P., Gerakines, P. A., Lacy, J. H., Millar, T. J., Schutte, W. A., Tielens, A. G. G. M., Whittet, D. C. B., Boxhoorn, D. R., Kester, D. J. M., Leech, K., Roelfsema, P. R., Salama, A., Vandenbussche, B. 1996, A search for interstellar gas-phase CO_2. Gas:solid state abundance ratios, A&A, 315, L349–L352

van Dishoeck, E.F., Wright, C.M., Cernicharo, J., González-Alfonso, E., Helmich, F.P., de Graauw, Th., Vandenbussche, B. 1998, The ISO-SWS 2.4-45.2 μm spectrum toward Orion IRc2, ApJ, 502, L173–L176

van Kerckhoven, C., Hony, S., Peeters, E., Tielens, A. G. G. M., Allamandola, L. J., Hudgins, D. M., Cox, P., Roelfsema, P. R., Voors, R. H. M., Waelkens, C., Waters, L. B. F. M., Wesselius, P. R. 2000, The C-C-C bending modes of PAHs: a new emission

plateau from 15 to 20 μm, A&A, 357, 1013–1019
van Winckel, H., Reyniers, M. 2000, A homogeneous study of the s-process in the 21 μm carbon-rich post-AGB objects, A&A, 354, 135–149
Vardya, M.S., de Jong, T., Willems, F.J. 1986, IRAS Low-Resolution Spectrograph observations of silicate and molecular SiO emission in Mira variables, ApJ, 304, L29–L32
Verstraete, L., Puget, J.L., Falgarone, E., Drapatz, S., Wright, C.M., Timmermann, R. 1996, SWS spectroscopy of small grain features across the M17-Southwest photodissociation front, A&A, 315, L337–L340
von Helden, G., Tielens, A.G.G.M., van Heijnsbergen, D., Duncan, M.A., Hony, S., Waters, L.B.F.M., Meijer, G. 2000, Science, 288, 313–316
Voors, R.H.M. 1999, Ph.D. Thesis, Universiteit Utrecht.
Vriend, W.-J. 2000, Masters Thesis, Rijksuniversiteit Groningen
Waelkens, C., Waters, L.B.F.M., de Graauw, Th., Huygen, E., Malfait, K., Plets, H., Vandenbussche, B., Beintema, D. A., Boxhoorn, D. R., Habing, H. J., Heras, A. M., Kester, D. J. M., Lahuis, F., Morris, P. W., Roelfsema, P. R., Salama, A., Siebenmorgen, R., Trams, N. R., van der Bliek, N. R., Valentijn, E. A., Wesselius, P. 1996, SWS observations of young main-sequence stars with dusty circumstellar disks, A&A, 315, L245–L248
Waters, J.W., Gustincic, J.J., Kakar, R.K., Kuiper, T.B.H., Roscoe, H.K., Swanson, P.N., Rodriguez-Kuiper, E.N., Kerr, A.R., Thaddeus, P. 1980, Observations of interstellar H_2O emission at 183 GHz, ApJ, 235, 57–62
Waters, L.B.F.M., Waelkens, C., van der Hucht, K.A., Zaal, P.A., eds. 1998, ISO's View on Stellar Evolution (Kluwer, Dordrecht), Astrophys. Spa. Sc. vol. 255
Waters, L.B.F.M., Beintema, D.A., Zijlstra, A.A., de Koter, A., Molster, F. J., Bouwman, J., de Jong, T., Pottasch, S. R., de Graauw, Th. 1998a, Crystalline silicates in planetary nebulae with [WC] central stars, A&A, 331, L61–L64
Waters, L.B.F.M., Cami, J., de Jong, T., Molster, F. J., van Loon, J. Th., Bouwman, J., de Koter, A., Waelkens, C., Van Winckel, H., Morris, P. W. 1998b, An oxygen-rich dust disk surrounding an evolved star in the Red Rectangle, Nature, 391, 868
Watson, D.M., Genzel, R., Townes, C.H., Storey, J.W.V. 1985, Far-infrared emission lines of CO and OH in the Orion-KL molecular shock, ApJ, 298, 316–327
Weinreb, S., Barrett, A.H., Meeks, M.C., Henry, J.C. 1963, Nature, 200, 829
Whittet, D.C.B. 1992, Dust in the Galactic Environment (IOP, Bristol)
Willems, F.J. 1988, IRAS low-resolution spectra of cool carbon stars, A&A, 203, 51–70
Willner, S.P., Gillett, F.C., Herter, T.L., Jones, B., Krassner, J., Merrill, K. M., Pipher, J. L., Puetter, R. C., Rudy, R. J., Russell, R. W., Soifer, B. T. 1982, Infrared spectra of protostars - composition of the dust shells, ApJ, 253, 174–187
Willner, S.P., Soifer, B.T., Russell, R.W., Joyce, R.R., Gillett, F.C., 1977, 2 to 8 micron spectrophotometry of M82, ApJ, 217, L121–L124
Wilson, R.W., Jefferts, K.B., Penzias, A.A. 1970, Carbon monoxide in the Orion nebula, ApJ, 161, L43–L44
Wickramasinghe, D.T., Allen, D.A. 1980, The 3.4-micron interstellar absorption feature, Nature, 287, 518
Wright, C.M. 2000, Observations of molecular hydrogen in shocks and PDRs with the Infrared Space Observatory, in Astrochemistry: From Molecular Clouds to Planetary Systems, IAU Symposium 197, eds. Y.C. Minh & E.F. van Dishoeck (ASP, San Francisco), p. 177–190
Wright, C.M., van Dishoeck, E.F., Cox, P., Sidher, S.D., Kessler, M.F. 1999, ISO-LWS detection of the 112 μm HD $J = 1 \rightarrow 0$ Line toward the Orion Bar, ApJ, 515, L29–L32
Wright, C.M., van Dishoeck, E.F., Black, J.H., Feuchtgruber, H., Cernicharo, J., González-Alfonso, E., de Graauw, Th. 2000, ISO-SWS observations of pure rotational H_2O absorption lines toward Orion-IRc2, A&A, 358, 689–700
Wright, E.L., Mather, J.C., Bennett, C.L., Cheng, E. S., Shafer, R. A., Fixsen, D. J., Eplee, R. E., Jr., Isaacman, R. B., Read, S. M., Boggess, N. W., Gulkis, S., Hauser, M.

G., Janssen, M., Kelsall, T., Lubin, P. M., Meyer, S. S., Moseley, S. H., Jr., Murdock, T. L., Silverberg, R. F., Smoot, G. F., Weiss, R., Wilkinson, D. T. 1991, Preliminary spectral observations of the Galaxy with a 7 deg beam by the Cosmic Background Explorer (COBE), ApJ, 381, 200–209

Xie, T., Allen, M., Langer, W.D. 1995, Turbulent diffusion and its effects on the chemistry of molecular clouds, ApJ, 440, 674–685

Yun, J., Liseau, R. 1998, Star Formation with the Infrared Space Observatory, ASP vol. 132 (ASP, San Francisco)

Zmuidzinas, J., Blake, G.A., Carlstrom, J., Keene, Jocelyn, Miller, D., Schilke, P., Ugras, N. G. 1995, Submillimeter spectroscopy of interstellar hydrides, In Proceedings of the Airborne Astronomy Symposium, ed. M.R. Haas, J.A. Davidson, E.F. Erickson, (ASP, San Francisco), p. 33–40

Zuckerman, B., Forveille, T., Kastner, J.H. 1995, Inhibition of giant planet formation by rapid gas depletion around young stars, Nature, 373, 494